ANNUAL REVIEWS

Annual Review of Marine Science

The Variable Southern Ocean Carbon Sink

Nicolas Gruber,[1] Peter Landschützer,[2] and Nicole S. Lovenduski[3]

[1]Environmental Physics, Institute of Biogeochemistry and Pollutant Dynamics, ETH Zurich, 8092 Zurich, Switzerland; email: nicolas.gruber@env.ethz.ch

[2]Max Planck Institute for Meteorology, 20146 Hamburg, Germany

[3]Department of Atmospheric and Oceanic Sciences and Institute of Arctic and Alpine Research, University of Colorado, Boulder, Colorado 80309, USA

Annu. Rev. Mar. Sci. 2019. 11:159–86

First published as a Review in Advance on September 13, 2018

The *Annual Review of Marine Science* is online at marine.annualreviews.org

https://doi.org/10.1146/annurev-marine-121916-063407

Keywords

Southern Ocean, ocean carbon sink, decadal variability, anthropogenic carbon, natural carbon

Abstract

The CO_2 uptake by the Southern Ocean (<35°S) varies substantially on all timescales and is a major determinant of the variations of the global ocean carbon sink. Particularly strong are the decadal changes characterized by a weakening period of the Southern Ocean carbon sink in the 1990s and a rebound after 2000. The weakening in the 1990s resulted primarily from a southward shift of the westerlies that enhanced the upwelling and outgassing of respired (i.e., natural) CO_2. The concurrent reduction in the storage rate of anthropogenic CO_2 in the mode and intermediate waters south of 35°S suggests that this shift also decreased the uptake of anthropogenic CO_2. The rebound and the subsequent strong, decade-long reinvigoration of the carbon sink appear to have been driven by cooling in the Pacific Ocean, enhanced stratification in the Atlantic and Indian Ocean sectors, and a reduced overturning. Current-generation ocean models generally do not reproduce these variations and are poorly skilled at making decadal predictions in this region.

1. INTRODUCTION

The Southern Ocean, defined here as the vast region south of 35°S that encircles Antarctica without any impeding continents, has captivated human imagination ever since its discovery a few centuries ago. But it was the recognition of the Southern Ocean's crucial importance for the global carbon cycle and climate a few decades ago (McElroy 1983, Sarmiento & Toggweiler 1984, Siegenthaler & Wenk 1984) that catapulted it to the forefront of scientific interest (see, e.g., Morrison et al. 2015). Even though this region covers only approximately 20% of the world's ocean's surface, it is responsible for approximately 40% of the global oceanic uptake of anthropogenic CO_2 (Caldeira & Duffy 2000, Orr et al. 2001, Mikaloff Fletcher et al. 2006, DeVries 2014) and for approximately 75% of the excess heat generated in the Earth system (Frölicher et al. 2015). Furthermore, this region acts as the key gatekeeper controlling the supply of nutrients to the low-latitude oceans and thus the magnitude of low-latitude productivity in the past, present, and future (Matsumoto et al. 2002, Sarmiento et al. 2004, Moore et al. 2018).

The ability to observe the Southern Ocean has been utterly incommensurate with its importance (e.g., Majkut et al. 2014). As a result, our understanding of its dynamics, particularly its temporal variability, has remained comparatively poor. Thus, the community was taken by surprise when the first evidence—mainly model based—emerged that the Southern Ocean carbon sink might have slackened considerably during the 1990s (Le Quéré et al. 2007, Lovenduski et al. 2008). Of particular concern was that the likely cause of this slackening was a trend toward a more southerly position of the westerly winds, i.e., a trend that had been predicted to continue in a warming world (Gillett & Thompson 2003, Miller et al. 2006). This would imply that the Southern Ocean sink might have already saturated (Le Quéré et al. 2007). And since this weakening trend was not compensated for in the other oceanic basins, the uptake of the whole ocean appeared to slow relative to the expected increase in uptake in response to the rise in atmospheric CO_2 (Wanninkhof et al. 2013, Landschützer et al. 2016) (see **Figure 1**). A reduced uptake would

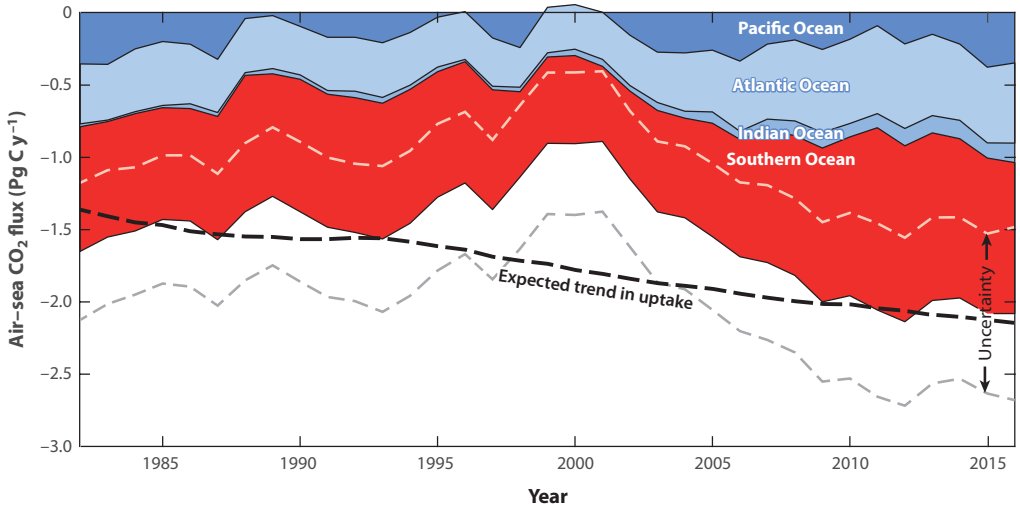

Figure 1

Temporal evolution of the global ocean sink for atmospheric CO_2 and the contributions of each basin (separated at 35°S). The area between the dashed gray lines indicates the uncertainty interval around the global mean. The dashed black line represents the expected uptake based on the increase in atmospheric CO_2 estimated from a hindcast simulation with an ocean biogeochemistry model (Graven et al. 2012) scaled to the global contemporary CO_2 flux estimated by Gruber et al. (2009). Negative fluxes indicate a sink for atmospheric CO_2. Figure adapted and updated from Landschützer et al. (2016).

have serious consequences for Earth's climate since the whole ocean may no longer provide the critically important sink for anthropogenic CO_2 emitted into the atmosphere due to fossil fuel burning and land use change (Sabine et al. 2004, Gruber et al. 2009, Khatiwala et al. 2013, Le Quéré et al. 2018).

But as the observational databases (Bakker et al. 2016) and analysis techniques (Landschützer et al. 2013; Rödenbeck et al. 2014, 2015) improved over time, it became evident that the Southern Ocean carbon sink has not saturated at all. Instead, a growing number of (mostly observational) studies suggest that, after reaching a minimum around the turn of the millennium, the Southern Ocean carbon sink strengthened rapidly, regaining its full strength in less than 10 years (Landschützer et al. 2015, Munro et al. 2015, Gregor et al. 2018). The reinvigoration of this carbon sink together with a substantial increase in the sinks of the other ocean basins during the first decade of the millennium brought the global ocean sink strength back to the level expected from the increase in atmospheric CO_2 (Landschützer et al. 2016) (**Figure 1**).

Thus, the view emerging from these more recent studies is that, on timescales of a few decades or longer, the ocean carbon sink appears to have been operating at a relatively constant strength—i.e., it has been taking up approximately the same proportion of the total anthropogenic CO_2 emissions in the last few decades as it has been since the beginning of the industrial emissions (~30%) (Sabine et al. 2004, Gruber et al. 2018, Le Quéré et al. 2018). This is consistent with the observation that, when analyzing time series of the air–sea difference of the partial pressure of CO_2 (pCO_2) over a period of two decades or longer, the majority of the oceanic regions emerge as having no significant trend (e.g., Fay & McKinley 2013), signifying no major shift in uptake. At the same time, the evidence is strengthening that the ocean carbon sink is characterized by a substantial amount of decadal variability and that this variability is confounding trend analyses based on data covering two decades or less (Fay et al. 2014; McKinley et al. 2016, 2017). But this high level of decadal variability, especially in the Southern Ocean, is found only in observation-based analyses (Rödenbeck et al. 2014, Landschützer et al. 2015, Ritter et al. 2017), not in simulations from the majority of ocean models (Lenton et al. 2013).

These large fluctuations in global ocean carbon uptake, particularly those in the Southern Ocean, give rise to many questions. First, are these decadal variations real or just an artifact of methods that attempt to extrapolate information from the still relatively sparse observational bases to the entire globe? Second, if those fluctuations are real, what mechanisms are driving these unexpectedly large decadal variations? Third, how well are these decadal variations captured by the current generation of models, and what does this imply for the future? And fourth, are these variations predictable?

Here, we address these questions by reviewing what is known and not known about the recent trends and variations of the Southern Ocean carbon sink. We focus on the mechanisms and the connection of these surface processes with ocean-interior changes in carbon content. A thorough discussion of these issues requires a good foundation, which we provide by first reviewing the time-mean fluxes, the processes controlling them, and the seasonal cycle. We also provide a short overview of the main methods that have been used to quantify the Southern Ocean carbon sink, with a focus on those that underlie this synthesis.

2. BACKGROUND

2.1. Mean Sources and Sinks of CO_2 in the Southern Ocean

The crucial role of the Southern Ocean for the global carbon cycle is a direct consequence of its unique circulation. Unblocked by land, the strong winds of the Roaring Forties and Furious

Fifties in the Southern Hemisphere not only propel the world's largest oceanic current—the Antarctic Circumpolar Current (Munk & Palmén 1951, Johnson & Bryden 1989)—but also cause a meridional overturning circulation that plays a key role in the closure of the global deep circulation (e.g., Marshall & Speer 2012, Morrison et al. 2015). Driving an intense surface divergence through Ekman transport, these winds generate strong upwelling in the region immediately south of the Antarctic Polar Front, at approximately 60°S. This upwelling brings to the surface waters that are high in dissolved inorganic carbon (DIC) (right side of **Figure 2*a***), which is a consequence of the old age of these upwelled waters, reflecting their origin in the deep Atlantic, Indian, and Pacific Oceans. As a result, they contain a large amount of DIC stemming from the remineralization of organic matter and the dissolution of biogenic $CaCO_3$, reflecting variations in DIC that arise from natural processes (Sarmiento & Gruber 2006). We thus refer to this component of DIC as natural CO_2. The old age of these waters also implies that they were last in contact with the atmosphere in preindustrial times, when atmospheric CO_2 had not yet been perturbed by anthropogenic CO_2 emissions. Thus, they contain essentially no anthropogenic CO_2 (Gruber 1998, McNeil et al. 2001, Lee et al. 2003, Carter et al. 2017), the signal imparted to the ocean by the increase in atmospheric CO_2 (Gruber et al. 2009, McNeil & Matear 2013) (left side of **Figure 2*a***).

Once these waters reach the surface, they tend to be either pushed southward, where they are transformed into very cold and relatively fresh Antarctic Bottom Water through cooling and freshening by the atmosphere and the land and sea ice, or transported northward by the Ekman-driven transport (red arrows in **Figure 2*a***). The former pathway, i.e., the lower cell (Marshall & Speer 2012), is subject to only a relatively limited amount of exchange of CO_2 with the atmosphere owing, in part, to the strong physical blocking of the exchange by sea ice (Hoppema et al. 2001, Butterworth & Miller 2016). By contrast, strong air–sea fluxes are associated with the northward pathway, i.e., the upper cell.

As these waters flow northward and before they are transformed into intermediate waters and later subducted around 40–50°S, they tend to lose a substantial amount of their natural CO_2 by outgassing (right side of **Figure 2*a***). This is largely a consequence of the inefficiency of the biological pump in stripping out the CO_2 (Mikaloff Fletcher et al. 2007). The latter reflects the strong light and micronutrient (iron) limitation of phytoplankton in the Southern Ocean, which prevents them from reaching the potential provided by the high macronutrient content of these upwelled waters (Boyd et al. 2000, Watson et al. 2000). The outgassing of natural CO_2 south of 44°S amounts to approximately 0.4 Pg C y^{-1}, making it one of the largest sources of natural CO_2 (Mikaloff Fletcher et al. 2007). In fact, this outgassing is thought to have been an important contributor to the preindustrial south-to-north gradient in atmospheric CO_2 (Gloor et al. 2003).

North of 44°S, the Southern Ocean is a very strong sink for natural CO_2, driven mainly by the cooling of the southward-transported subtropical waters that eventually become mode waters (Gruber et al. 2009) (right side of **Figure 2*a***). Thus, the distribution of the air–sea fluxes of natural CO_2 in the Southern Ocean consists of an inner ring of strong outgassing and an outer ring characterized by strong uptake (right side of **Figure 2*a***). Integrated from the coast of Antarctica to 35°S, these two regions compensate for each other nearly perfectly, leading to a near-zero net uptake of natural CO_2.

In contrast to natural CO_2, the entire Southern Ocean south of 35°S is a sink for anthropogenic CO_2 (left side of **Figure 2*a***), summing to a total uptake of approximately 1 Pg C y^{-1} (Mikaloff Fletcher et al. 2006, DeVries 2014). The majority of this uptake occurs between the Antarctic Polar Front and the Subpolar Front, leading to a distinct ring of high-uptake fluxes at the latitudes between 45°S and 55°S. This uptake is associated with the upper cell that transports recently upwelled waters with a very low initial anthropogenic CO_2 concentration northward and exposes them to the atmosphere in a region of high wind speeds, leading to high-uptake fluxes. The

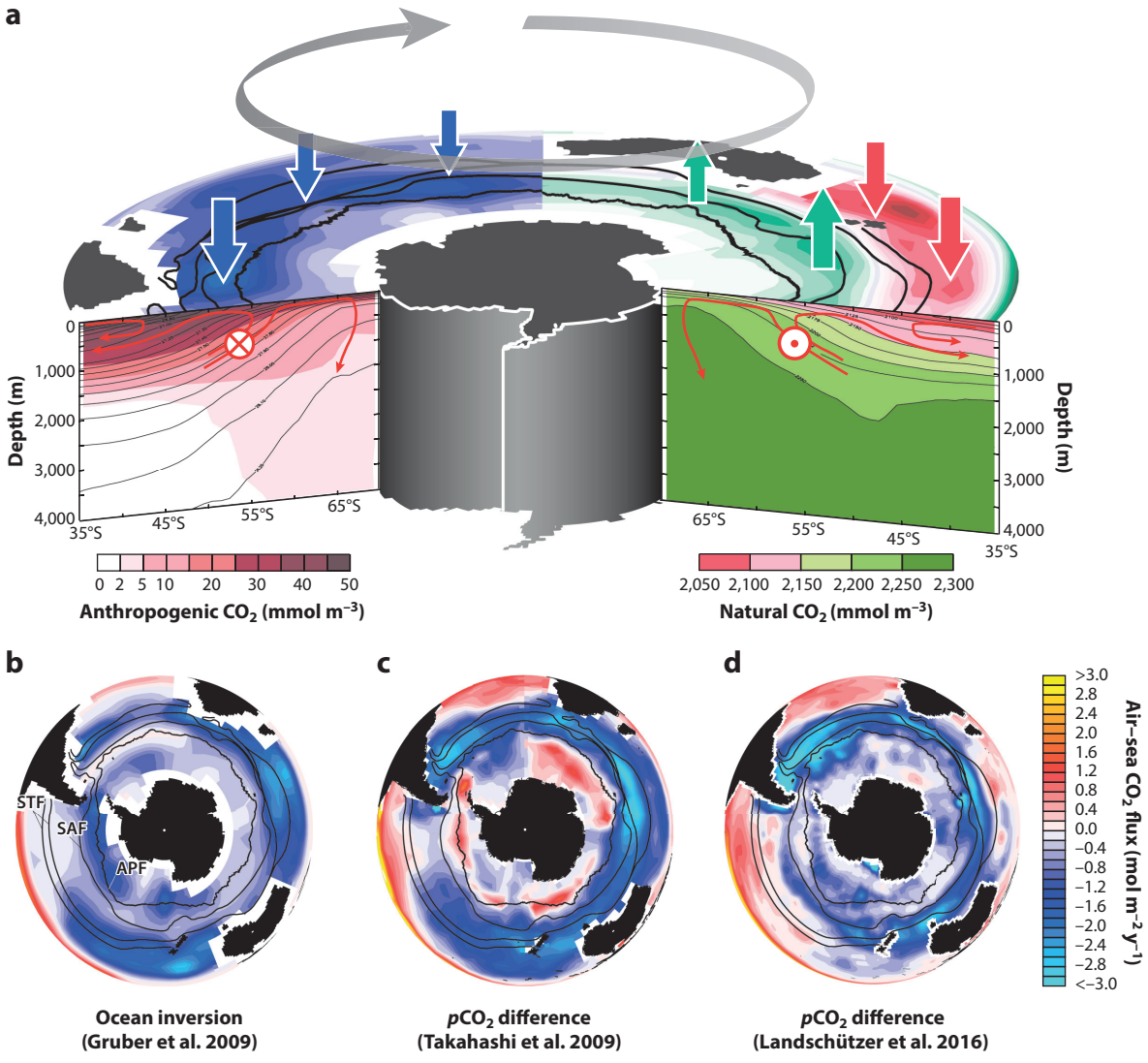

Figure 2

(*a*) Schematic diagram of the zonal mean overturning circulation of the Southern Ocean and the associated fluxes of anthropogenic (*left*) and natural (*right*) CO_2 based on the ocean inversion estimates of Gruber et al. (2009). The vertical sections depict the distribution of anthropogenic CO_2 (*left*) and dissolved inorganic carbon (*right*) for 1994 (Key et al. 2004). The red circles indicate the Antarctic Circumpolar Current flowing into the plane (*circle with X*) or out of the plane (*circle with dot*) formed by the respective sections. (*b*) Inverse estimate of the contemporary air–sea CO_2 flux (nominal year 1995), representing the sum of the natural and anthropogenic CO_2 fluxes shown in panel *a* (Gruber et al. 2009). (*c*) pCO_2-based estimate of the contemporary air–sea CO_2 flux using the product of Takahashi et al. (2009) (nominal year 2000). (*d*) The same as panel *c* but for the product of Landschützer et al. (2016) (nominal year 2000). In all panels, the black lines show the dominant fronts in the Southern Ocean, moving equatorward from Antarctica: the Antarctic Polar Front (APF), Subantarctic Front (SAF), and Southern and Northern Subtropical Fronts (STF).

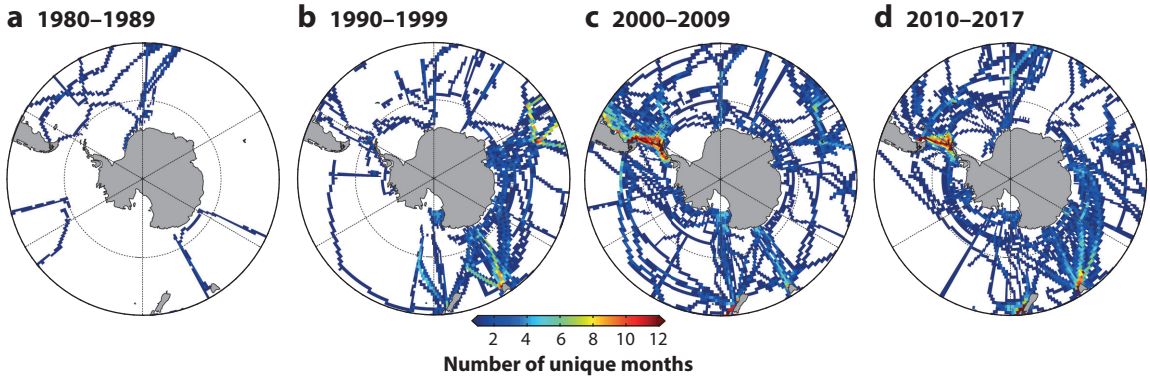

Figure 3

Polar stereographic maps of the distribution of surface-ocean pCO_2 observations in the Southern Ocean for (*a*) 1980–1989, (*b*) 1990–1999, (*c*) 2000–2009, and (*d*) 2010–2017. The colors indicate the number of unique months with observations for each 1° × 1° pixel.

upper cell then transports this anthropogenic CO_2 to depth through the subduction of mode and intermediate waters (Sabine et al. 2004, Mikaloff Fletcher et al. 2006, Ito et al. 2010, Sallée et al. 2012, Bopp et al. 2015). In fact, this conduit, together with the additional anthropogenic CO_2 that it receives from the conversion of southward-transported subtropical waters into mode waters (Gruber et al. 2009, Iudicone et al. 2016), explains why the Southern Ocean is responsible for such a large fraction of the global uptake of anthropogenic CO_2 (Mikaloff Fletcher et al. 2006, DeVries 2014, Frölicher et al. 2015). Approximately two-thirds of this uptake is actually stored in the region south of 35°S; the other third is transported northward and stored in the thermocline of the midlatitudes (Mikaloff Fletcher et al. 2006, DeVries 2014, Bopp et al. 2015).

The spatial superpositioning of the natural and anthropogenic CO_2 fluxes in the contemporary flux leads to a relatively strong and broad uptake band between approximately 55°S and 35°S, with the northern part driven by the uptake of natural CO_2 and the southern part driven by the uptake of anthropogenic CO_2 overcompensating for the outgassing of natural CO_2 there (**Figure 2*b–d***). South of the Polar Front, the different estimates agree less well, reflecting the paucity of measurements there (**Figure 3**). Most likely, this region is currently a small source, which is also supported by recent measurements based on biogeochemical floats (Gray et al. 2018, Williams et al. 2018).

2.2. Methods for Estimating Carbon Sources and Sinks

A broad palette of methods, including observations and models, have been used to assess the sources and sinks of the Southern Ocean. Each has its own particular strengths and limitations, which we review next, starting with observations.

Observations of surface-ocean pCO_2, primarily from underway programs on research ships and ships of opportunity (Bakker et al. 2016), are by far the most important observational constraint for the sources and sinks of CO_2 in the ocean. But even though dedicated programs such as the Drake Passage time-series project (Munro et al. 2015) have substantially increased the number of observations in the Southern Ocean in recent decades, the data remain sparse in time and space (**Figure 3**), largely because of the logistical and experimental challenges associated with obtaining observations in this remote and often hostile environment. The sparseness of the data requires sophisticated interpolation methods to extend the data in time and space, ranging from rather

simple spatial interpolation to complex machine-learning-based approaches (Rödenbeck et al. 2015). Furthermore, the determination of the air–sea CO_2 flux based on ocean pCO_2 observations requires an estimation of the gas transfer velocity, which is associated with considerable uncertainty, especially of a systematic nature (Wanninkhof et al. 2009). As a result, the pCO_2-based method inherits these (systematic) uncertainties as well. While they matter less when assessing the interannual to decadal variability of the air–sea CO_2 transfer, they are a substantial concern when discussing the time-mean fluxes.

In comparison with the abundant surface pCO_2 observations, there are many fewer observations of ocean-interior changes in DIC. Most cruises have sampled the Southern Ocean in the meridional direction, with only a handful having taken measurements along zonal lines (Talley et al. 2016; see also GO-SHIP 2017). Although the sampling coverage is high along the lines, the individual lines are far apart, requiring spatial and temporal interpolation techniques. Furthermore, the observed change in DIC between two occupations of the same line represents the sum of changes in both natural and anthropogenic CO_2, with the former reflecting mostly ocean-interior redistributions of DIC. In the past, the main interest has been detecting the part of the signal that is connected to the uptake of anthropogenic CO_2 from the atmosphere. As a consequence, several estimates are available for the ocean-interior change in anthropogenic CO_2 (Wanninkhof et al. 2010, Kouketsu & Murata 2014, Woosley et al. 2016, Carter et al. 2017, Gruber et al. 2018), while no estimate is available for the net ocean-interior change in natural CO_2.

All of the methods that attempt to identify the anthropogenic CO_2 signal rely on the fact that the ocean-interior changes in DIC tend to be tightly associated with changes in many other biogeochemical and physical variables, while an anomalous uptake of CO_2 from the atmosphere tends to change only DIC. This provides an opportunity to extract the air–sea CO_2 signal by investigating anomalies in the relationship between DIC and these biogeochemical and physical variables. This can be achieved by defining quasi-conservative tracers, such as C^* (Gruber et al. 1996, Gruber & Sarmiento 2002), or by using linear regression methods (Wallace 2001). From those latter methods, the extended multiple linear regression (eMLR) technique was developed (Friis et al. 2005) to specifically identify the change in DIC associated with the uptake of anthropogenic CO_2. The eMLR technique has been used extensively [see also the review by Sabine & Tanhua (2010)] and has been recently expanded and modified [eMLR(C^*)] to estimate global changes in the ocean-interior DIC associated with the uptake and storage of anthropogenic CO_2 (Clement & Gruber 2018).

In addition to observations, models have played an important role in the discussion of the Southern Ocean CO_2 fluxes and their variability. A range of modeling approaches have been used, including hindcast simulations conducted with ocean physical and biogeochemical models forced with the observed fluxes of momentum, heat, and fresh water from the past (e.g., Lenton & Matear 2007; Lovenduski et al. 2007, 2008). This is also the main approach taken by the Global Carbon Project to constrain the ocean carbon sink variability (Le Quéré et al. 2018).

Inverse models are becoming an increasingly important constraint as well (Gruber & Doney 2009), as the optimization of a model with observations enables one to combine the main strengths of the two methods, although gaps and errors in the observations as well as persistent model biases put strong limits on this approach. The first applications of such inverse methods were essentially limited to estimating the steady-state fluxes of natural and anthropogenic CO_2, since the observations were insufficient to study the impact of climatic variability (Gloor et al. 2003; Mikaloff Fletcher et al. 2006, 2007; Waugh et al. 2006; Gruber et al. 2009; Khatiwala et al. 2009). More recently, time-dependent inversion schemes have become available, but these rely largely on optimizing a numerical model of ocean circulation with hydrographic observations such as temperature, salinity, and the concentration of chlorofluorocarbons (CFCs), resulting in

an optimized ocean transport model that is then used in forward mode to compute the ocean carbon cycle, including the air–sea CO_2 fluxes (DeVries 2014, DeVries et al. 2017, Verdy & Mazloff 2017). A related approach that relies on atmospheric CO_2 data is the use of atmospheric CO_2 inversions (e.g., Rödenbeck et al. 2014), a method that played a key role in uncovering the large decadal variability in the Southern Ocean carbon sink (Le Quéré et al. 2007).

Fully coupled ocean–atmosphere models represent another category of forward models, but because they generate their own stochastic weather, the results of such model simulations can be compared only partially with observations. However, they provide a glimpse into the future (Sarmiento et al. 1998, Lovenduski & Ito 2009). In addition, through simulations run with and without change in anthropogenic forcing, as well as through the use of large ensembles, they are providing a much better understanding of which part of the variability is driven by internal (stochastic) processes and which part is a true trend driven by anthropogenic climate change (e.g., McKinley et al. 2016, 2017).

In this review, we rely primarily on surface-ocean pCO_2 observations and ocean-interior measurements and complement these data with model-based results. Concretely, for surface-ocean pCO_2, we use the most recent results of a two-step neural network method [the self-organizing map–feed-forward neural network (SOM-FFN) approach] that was first developed by Landschützer et al. (2013) and later refined and updated (Landschützer et al. 2016). We use here the most updated version prepared for the 2018 global carbon budget, which employed data from the Surface Ocean CO_2 Atlas Database Version 5 (Bakker et al. 2017), but the methods are identical to those of Landschützer et al. (2016). We contrast the results from this method with those of the most recent version of the mixed-layer mapping method of Rödenbeck et al. (2014). While these two methods differ greatly, they both perform best when compared against a few benchmark tests (Rödenbeck et al. 2015). For the ocean interior, we rely on the reconstructed changes in anthropogenic CO_2 between 1994 and 2007 for the Southern Ocean (Gruber et al. 2018). These results were obtained by applying the eMLR(C^*) method (Clement & Gruber 2018) to the recent observations synthesized in Global Ocean Data Analysis Project Version 2 (GLODAPv2) (Olsen et al. 2016). For the models, we use the hindcast simulation results of seven global ocean biogeochemical models (Doney et al. 2009, Buitenhuis et al. 2010, Ilyina et al. 2013, Séférian et al. 2013, Hauck et al. 2016, Schwinger et al. 2016, Law et al. 2017) conducted for the Global Carbon Project (Le Quéré et al. 2018). We also rely on the time-resolving inverse studies of DeVries et al. (2017), as well as the large-ensemble modeling studies with the fully coupled Earth system model from the National Center for Atmospheric Research (Kay et al. 2015).

3. THE VARIABILITY OF THE SOUTHERN OCEAN CARBON SINK

The air–sea CO_2 fluxes reconstructed from surface-ocean pCO_2 observations using the SOM-FFN method (Landschützer et al. 2016) show strong variations in Southern Ocean carbon uptake over the last three decades (**Figure 4*a***). These variations in fluxes are driven primarily by variations in surface-ocean pCO_2, as shown by the strong correspondence of these variations with those of the fluxes. The dominant mode of variability is the seasonal cycle, followed by a long-term trend toward a stronger sink (more negative flux) that is close to that expected from the increase in atmospheric CO_2 (see also **Figure 1**). Superimposed on this long-term trend is a substantial decadal variability signal that consists of a period of a strengthening sink in the 1980s, a period of a strongly weakening sink in the 1990s, and a period of a strongly reinvigorating sink in the first decade of the twenty-first century. Since approximately 2010, the sink strength has remained strong and unchanged overall. This high variability suggests that the carbon cycle in the Southern Ocean responds sensitively to climate variability on all timescales. In the following, we first discuss

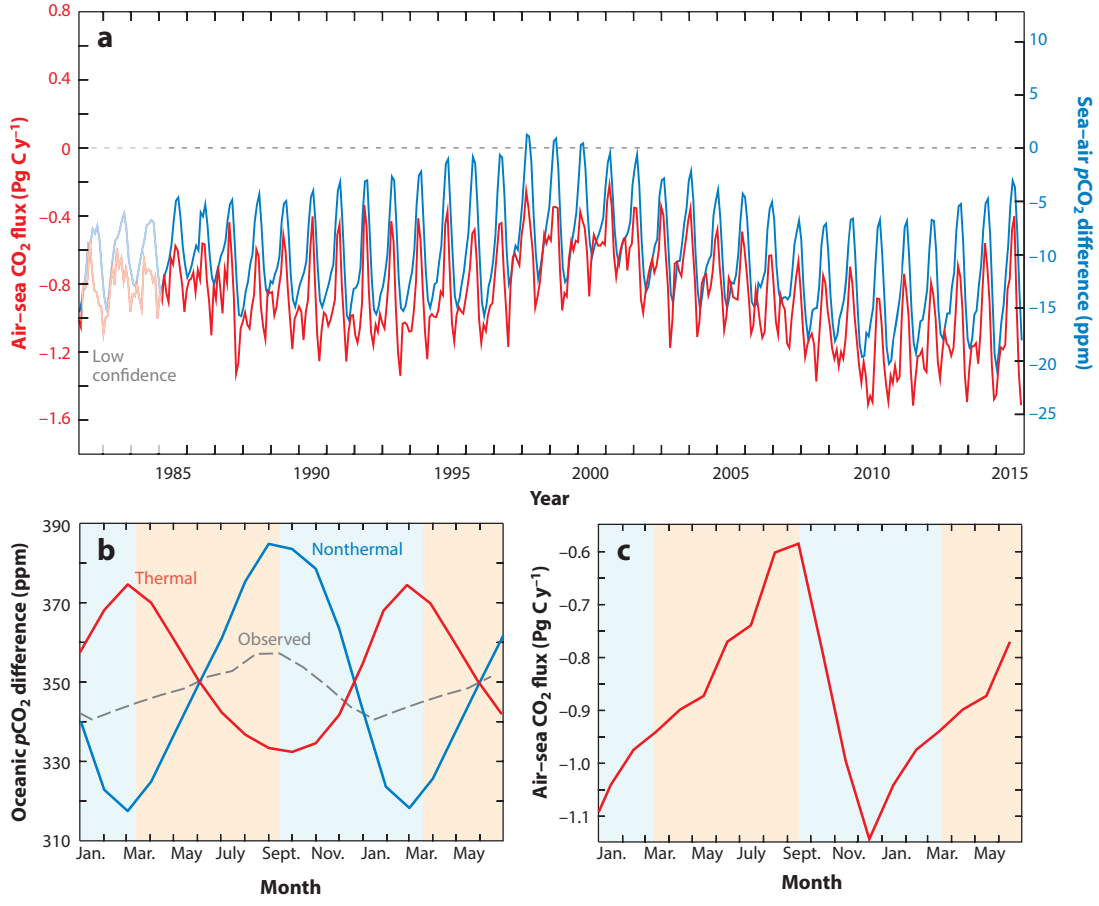

Figure 4

Variability of the Southern Ocean carbon sink. (*a*) Time series of monthly integrated air–sea CO_2 fluxes (*red line*) and monthly averaged sea–air pCO_2 difference (*blue line*), as inferred from the self-organizing map–feed-forward neural network (SOM-FFN) method (updated from Landschützer et al. 2016) for the region south of 35°S. (*b*) Monthly climatology of the average surface-ocean pCO_2 and its thermal and nonthermal components. (*c*) Monthly climatology of the integrated air–sea CO_2 flux. The climatologies of the SOM-FFN-based estimates were computed for the period from 1985 through 2015 and represent the average of the region south of 35°S.

the seasonal cycle, its drivers, and its changes, and then turn our attention to the variations on interannual to decadal timescales, i.e., the timescale that has resulted in a substantial scientific debate in the last decade (Le Quéré et al. 2007, Landschützer et al. 2015, Mikaloff Fletcher 2015).

3.1. Seasonal Variations

Seasonal variations explain approximately 30% of the total variance in the air–sea CO_2 fluxes and a similar amount of the surface pCO_2 variations. The seasonality of the Southern Ocean is characterized by a minimum in uptake in late winter (September) followed by a rapid increase toward a maximum in uptake in early summer (January) (**Figure 4*c***). This seasonality in the flux is driven almost entirely by the seasonality of surface-ocean pCO_2 (**Figure 4*b***), since the seasonal changes in wind—and hence in the air–sea gas exchange coefficient—are small by comparison (Takahashi et al. 2009, 2012).

The late-winter maximum and early-summer minimum in surface-ocean pCO_2 is a typical seasonal cycle for the high latitudes (Takahashi et al. 2009, Landschützer et al. 2018). It is driven primarily by the nonthermal component, i.e., the part of the variations in surface-ocean pCO_2 that results from variations in the concentrations of DIC and alkalinity, which themselves are primarily a result of variations in biological activity and physical transport and mixing. This component can also be thought of as the variations that the surface-ocean pCO_2 would have if the temperature were held constant at the annual mean value. The thermal component, i.e., the component driven by variations in sea-surface temperature, is opposite in phasing, so the observed seasonal cycle in pCO_2 is actually the result of two strongly opposing influences (**Figure 4*b***). This separation is achieved by using the well-known thermal sensitivity of pCO_2 [approximately a 4% change in pCO_2 per degree Celsius change (Takahashi et al. 1993)] to compute the thermal component, and then taking the difference from the observed total to compute the nonthermal component (see, e.g., Sarmiento & Gruber 2006). Since the seasonal variations in alkalinity tend to be relatively small, the seasonality of the nonthermal component primarily reflects the seasonal cycle of DIC, with winter mixing bringing high-DIC waters to the surface and summer biological productivity drawing down DIC and hence pCO_2 (Gregor et al. 2018). The winter-to-summer warming opposes this drawdown, so the total seasonal cycle is the net balance of these two opposing processes.

The seasonal cycle has substantially changed over the past 35 years. Most important is the long-term increase in the seasonal amplitude, which amounts to an increase of 1.1 ± 0.3 ppm per decade in the winter minus the summer difference in sea-surface pCO_2 (Landschützer et al. 2018) for the region between 40°S and 65°S. This increase results primarily from the long-term increase in surface-ocean CO_2, which enhances the absolute magnitude of the seasonal cycle in pCO_2, as the same relative sensitivity to (for example) temperature now acts on a larger annual mean surface-ocean pCO_2 (Landschützer et al. 2018). An additional contribution stems from the increase in the surface-ocean buffer factor driven by ocean acidification, which leads to stronger seasonal variations in the sea-surface concentration of CO_2 for the same seasonal variations in surface DIC.

Ocean models tend to reproduce the observed seasonal variations in pCO_2 relatively poorly (Anav et al. 2013, Lenton et al. 2013, Kessler & Tjiputra 2016, Mongwe et al. 2018). In the case of the hindcast models, this is primarily a result of their inability to fully capture the complex interactions between winter mixing and summer productivity. In the case of the fully coupled Earth system models, it turns out that for the majority of them, the thermal component is too large, leading to a thermally dominated seasonal cycle, as opposed to the observed nonthermal dominance (Mongwe et al. 2018). Given that year-to-year variations are often driven by modifications of the seasonal cycle, modeling these variations is also likely be challenging.

3.2. Interannual to Decadal Variations

The strong decadal variations in the flux reconstructions from the SOM-FFN method (Landschützer et al. 2013) are also present in the mixed-layer-method-based reconstructions of Rödenbeck et al. (2014) (**Figure 5**). Particularly striking is that both methods agree on the presence of a strongly weakening sink trend in the 1990s followed by a reinvigoration past the turn of the millennium. This results in an extended period from approximately 1995 to 2010 where the Southern Ocean carbon sink was substantially smaller than predicted on the basis of the long-term climatological uptake and the increase in atmospheric CO_2, amounting to a cumulative reduction in uptake of approximately 4 ± 1 Pg C.

Although these estimates are subject to substantial uncertainty given the limited number of observations available in the region (**Figure 3**), these results are clearly supported by all but one of

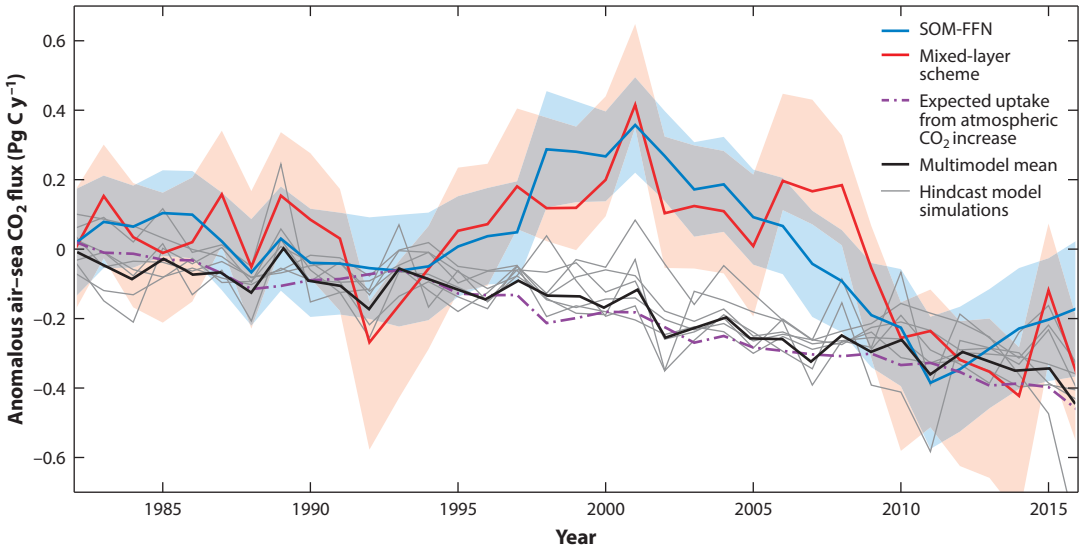

Figure 5

Decadal variability of the Southern Ocean carbon sink south of 35°S. Shown are the air–sea CO_2 flux anomalies, i.e., the deviations from the mean over the period 1982 to 2016, from the self-organizing map–feed-forward neural network (SOM-FFN) estimate (*blue*, updated from Landschützer et al. 2016) and from the mixed-layer scheme (*red*, updated from Rödenbeck et al. 2014). Negative values indicate a stronger sink. Also shown are the air–sea CO_2 flux anomalies from seven global biogeochemical models that contributed to the Global Carbon Project (Le Quéré et al. 2018) (i.e., Doney et al. 2009, Buitenhuis et al. 2010, Ilyina et al. 2013, Séférian et al. 2013, Hauck et al. 2016, Schwinger et al. 2016, and Law et al. 2017) (*gray lines*), the multimodel mean (*black line*), and the expected uptake based on the average of four of these simulations that did not consider climate variability (*dash-dotted purple line*). The shading indicates the uncertainty of the two observation-based products.

the pCO_2-based reconstructions collected by the Surface Ocean pCO_2 Mapping Intercomparison (SOCOM) initiative (Ritter et al. 2017) (**Figure 6*g***), irrespective of the method used to map the observations. This trend reversal also exists in the raw, uninterpolated data once the spatial bias has been corrected for (Fay et al. 2014). This conclusion is further supported by a detailed investigation of the data from the two most densely sampled regions—the Drake Passage (Munro et al. 2015) and the area south of Tasmania (Xue et al. 2015)—which suggests that the strong decadal trends are a robust feature of the surface-ocean data.

There is substantially less agreement with regard to the year-to-year variations (**Figure 5**). While the mixed-layer scheme of Rödenbeck et al. (2015) displays a substantial amount of variation from year to year, such variability is largely absent in the SOM-FFN-based reconstructions of Landschützer et al. (2016). As discussed by Landschützer et al. (2015), the mixed-layer scheme likely tends to overestimate the variations, while the neural network scheme perhaps tends to underestimate the variations through its tendency to smooth the final fields. More recently, Gregor et al. (2018) pointed out that the year-to-year variations are strongly driven by variations in seasonality, with the relative balance of winter mixing processes and summer biological processes playing a crucial role on interannual timescales but less so on decadal timescales.

The strong decadal variations identified in the observations are not reproduced in the hindcast simulations by the current generation of ocean biogeochemical models (**Figure 5**). Overall, the fluxes from these models tend to follow the expected increase in uptake rather closely, i.e., with only a slight indication of a saturation period in the 1990s and a reinvigoration period in the 2000s (**Figure 6*g***). But the spread is large and the signal much smaller than what the observations suggest.

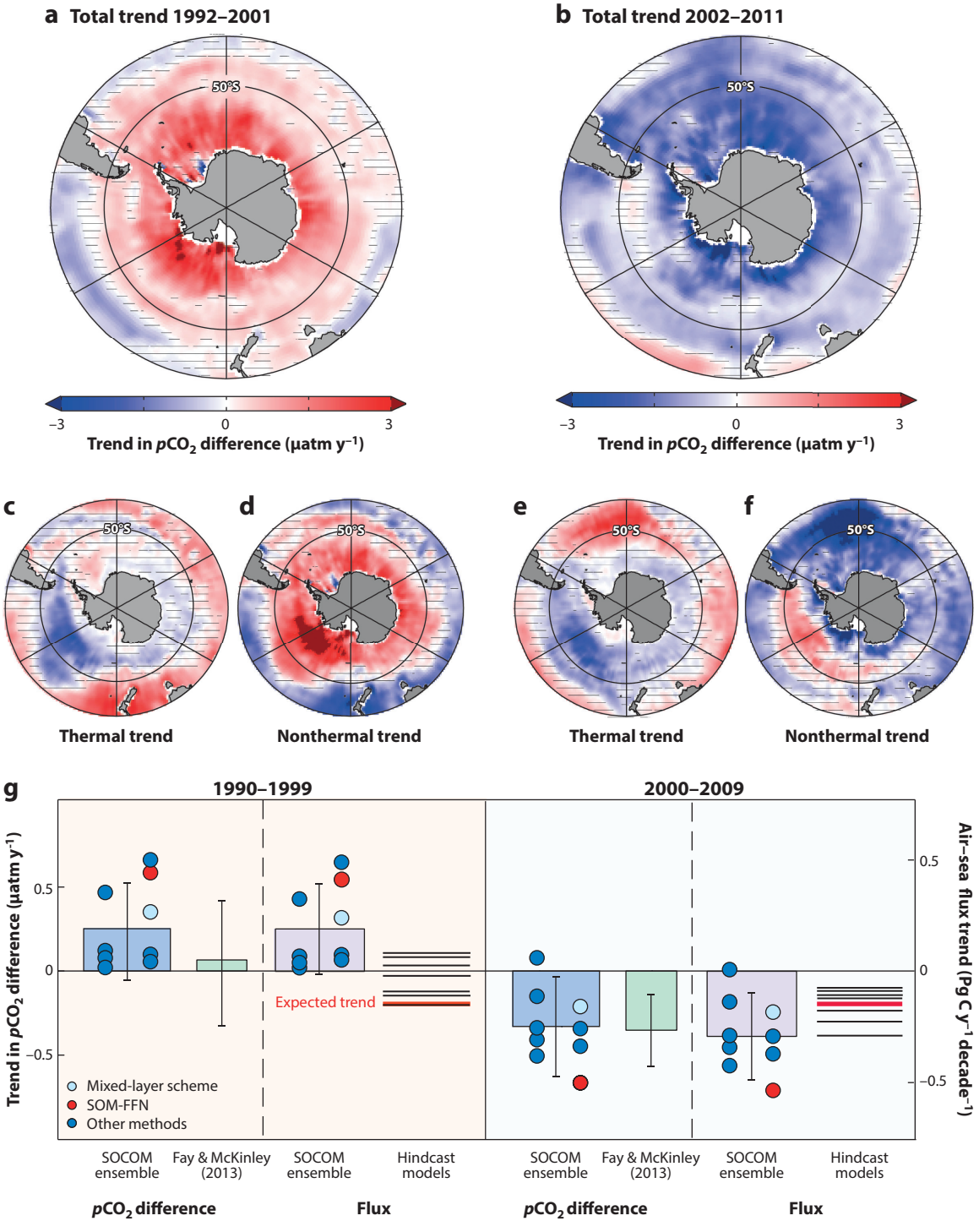

(*Caption appears on following page*)

Figure 6 (*Figure appears on preceding page*)

Decadal trends in the air–sea pCO_2 differences and air–sea CO_2 fluxes for the Southern Ocean. (*a*) Linear trend in the air–sea pCO_2 differences for 1992–2001 based on the self-organizing map–feed-forward neural network (SOM-FFN) method (Landschützer et al. 2016). (*b*) The same as panel *a* but for 2002–2011. (*c*,*d*) Linear trend in the thermal (panel *c*) and nonthermal (panel *d*) pCO_2 components for 1992–2001. (*e*,*f*) The same as panels *c* and *d* but for 2002–2011. Positive (*red*) trends in the air–sea pCO_2 differences indicate a faster increase of pCO_2 in the surface ocean than in the atmosphere (i.e., a decreasing sink), and negative (*blue*) trends indicate a faster increase in the atmosphere than in the surface ocean (i.e., an increasing sink). Hatching indicates areas where the linear trends are outside the 5% significance level ($p \geq 0.05$). (*g*) Estimated mean trends (ice weighted) in the air–sea pCO_2 difference of nine different pCO_2 mapping methods contained in the Surface Ocean pCO_2 Mapping Intercomparison (SOCOM) ensemble (Rödenbeck et al. 2015) for the Southern Ocean south of 30°S compared with the trend results reported by Fay & McKinley (2013). Also shown are the corresponding air–sea flux trends and their comparison with the trends inferred from seven hindcast model simulations that contributed to the Global Carbon Project (Le Quéré et al. 2018). The expected trend from the increase in atmospheric CO_2 is shown as the red line. Negative values indicate an increasing uptake of CO_2. The error bars represent the standard deviation (the standard deviations of Fay & McKinley 2013 are based on confidence intervals of 68.3%). Note that the two analysis periods are slightly shifted as a result of the choices made in the original publications. Panels *a*–*f* adapted and updated from Landschützer et al. (2015); panel *g* adapted and updated from Ritter et al. (2017).

In contrast to the near absence of decadal trends, these models simulate substantial interannual variations in the Southern Ocean air–sea CO_2 fluxes, but with little congruence among the different models. The reason for the poor performance has not been fully explained but is in line with the problems many of these models face in simulating the annual mean fluxes and the seasonal cycle with sufficient fidelity (Lenton et al. 2013, Jiang et al. 2014, Kessler & Tjiputra 2016).

Analyzing the spatial pattern of the trends and the relative contributions of the thermal and nonthermal components can provide some initial insights into the processes driving the decadal variations (**Figure 6*a*–*f***). A striking observation is that the decadal trends of pCO_2 differences in the 1990s and early 2000s from the SOM-FFN method are spatially rather homogeneous, with nearly the entire Southern Ocean south of approximately 40°S contributing to the anomalous pCO_2 differences and air–sea fluxes of CO_2. During the 1990s, the trend in the air–sea pCO_2 difference exceeded 1 μatm y^{-1} for nearly the entire region south of 50°S (**Figure 6*a***). During the first decade of the 2000s, the trend reversed to −1 μatm y^{-1} in magnitude, particularly in the Atlantic and Indian Ocean sectors (**Figure 6*b***), while the trends in the Pacific were relatively weak. Although the magnitude of the trends estimated by the SOM-FFN method are approximately twice as large as those of the multiproduct mean from the SOCOM ensemble (**Figure 6*g***), the spatial pattern of the trends in the SOCOM ensemble are very similar (Ritter et al. 2017).

The separation of the total trends into their thermal and nonthermal trend components shows a more complex pattern of change (**Figure 6*c*–*f***). During the 1990s, a spatially relatively homogeneous positive nonthermal trend clearly emerges at the main driver, with cooling in the Pacific sector partially compensating for the trend there. During the first decade of the 2000s, the cooling trend in the Pacific sector overwhelmed the positive nonthermal trend there, resulting in the entire Southern Ocean having a negative trend in air–sea pCO_2 difference (see also the discussion in Landschützer et al. 2015).

4. OCEAN-INTERIOR CHANGES

The large changes seen in the air–sea CO_2 fluxes must leave an impact on the ocean-interior distribution of DIC as well. However, carbon stocks are remeasured much less frequently in the ocean interior than they are at the surface. Furthermore, the anomalous fluxes are small relative to the large ocean-interior stocks of DIC, which makes the detection of the changes challenging. Furthermore, with the best analytical methods achieving an accuracy of approximately 1 μmol kg^{-1}, some changes are also too small to be measured, particularly at depth. At the moment,

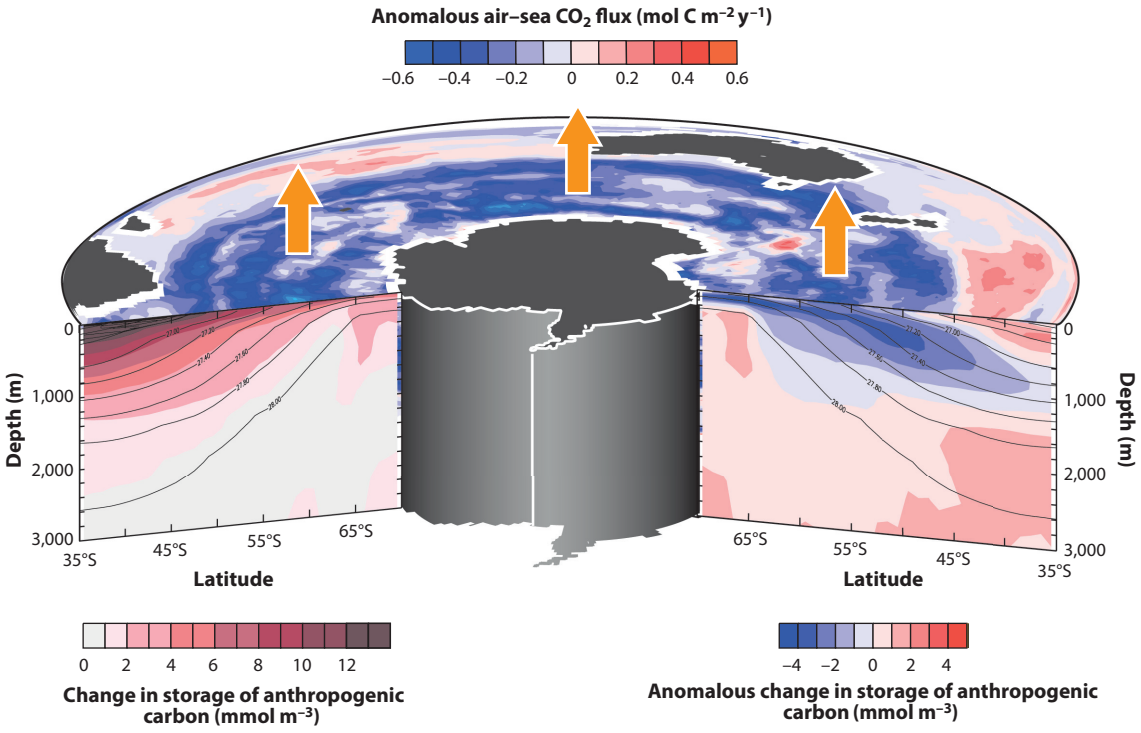

Figure 7

Diagram showing the changes in the oceanic storage of anthropogenic CO_2 (*left*) and their anomalies (*right*) between 1994 and 2007, together with the anomalous air–sea CO_2 fluxes (*top*) during this period. The isolines on the sections denote surfaces of equal neutral density. The zonally averaged changes in storage and their anomalies are from Gruber et al. (2018); the anomalous fluxes were computed from the SOM-FFN estimates (updated from Landschützer et al. 2016).

observation-based estimates of changes in ocean-interior DIC across the entire Southern Ocean are available only from 1994 to 2007 (Gruber et al. 2018). These estimates pertain only to the change in the ocean storage of anthropogenic CO_2, and no corresponding estimates of the change in the ocean storage of natural CO_2 are available.

The zonal mean changes in anthropogenic CO_2 between 1994 and 2007 reveal a substantial increase (**Figure 7**). The integrated change in storage south of 35°S amounts to a mean storage rate of 0.6 Pg C y^{-1}. This is substantially smaller than the mean uptake flux of anthropogenic CO_2 south of 35°S for this period of approximately 1 Pg C y^{-1} (see discussion in Section 2). This apparent discrepancy can be readily reconciled with the fact that the Southern Ocean exports a substantial amount of the taken-up anthropogenic CO_2 northward across 35°S (Mikaloff Fletcher et al. 2006, DeVries 2014). The vertical distribution of the change in anthropogenic CO_2 between 1994 and 2007 is very similar to the total amount of anthropogenic CO_2 present in the Southern Ocean in 1994 (compare with **Figure 2*a***), both of which reflect the distribution of a tracer that invades the ocean from the surface. Noteworthy in both distributions is the relatively shallow penetration south of 50°S followed by the much deeper penetration of the signal associated with the downward and northward transport of anthropogenic CO_2 with mode and intermediate waters.

The similarity between the changes in storage between 1994 and 2007 and the total amount of anthropogenic CO_2 present in 1994 is actually expected. It is a prediction of the transient

steady-state assumption (Gammon et al. 1982) that postulates that the changes in anthropogenic CO_2 at any location scale linearly with the amount of anthropogenic CO_2 already present. This transient steady-state assumption is applicable if the ocean circulation has remained relatively unchanged, the atmospheric CO_2 increase occurred close to exponentially, and the anthropogenic CO_2 perturbation has lasted long enough so that the ocean-interior distribution is in a transient steady state with respect to the atmospheric perturbation. This last assumption is well justified and has been successfully used many times in conjunction with oceanic uptake of anthropogenic CO_2 (e.g., Tanhua et al. 2007). The second assumption on the nature of the atmospheric CO_2 growth is only partially met, as atmospheric CO_2 indeed increased exponentially in the past few decades, but the decadally smoothed growth rates varied from approximately 1% before around 1950 to 2% thereafter. This limits the applicability of the transient steady-state assumption, but it turns out that the assumption works quite well for the 1994–2007 period, as the transition to the higher growth rate occurred many decades earlier (see discussion in Gruber et al. 2018). The fact that these latter two conditions are met and the change in storage is closely related to the total amount of anthropogenic CO_2 implies that the deviations from the first assumption of a constant ocean circulation cannot be overly large. This means that we can investigate these deviations of the actually reconstructed changes in storage of anthropogenic CO_2, i.e., the anthropogenic CO_2 storage anomalies.

To identify these anthropogenic CO_2 storage anomalies, we subtract the expected changes in anthropogenic CO_2 from the reconstructed changes. The expected changes are determined based on the predictions of the transient steady-state assumption from the amount of anthropogenic CO_2 already present in 1994 multiplied by a scaling factor of 0.28 (Gruber et al. 2018). This scaling factor was estimated from the fractional change in atmospheric CO_2 over this period, corrected for the change in the air–sea disequilibrium (Matsumoto & Gruber 2005) and the effect of the continuing decrease in ocean uptake efficiency owing to the ongoing rise in atmospheric CO_2 (Sarmiento & Gruber 2006). Thus, the anomalous changes in anthropogenic CO_2 storage are given by $\Delta_t C_{ant}^{anom} = \Delta_t C_{ant}^{meas} - 0.28 \cdot C_{ant}^{est,1994}$.

The resulting anthropogenic CO_2 storage anomalies are strongly negative in the mode and intermediate waters of the Southern Ocean (**Figure 7**). These anomalies have their origin near the surface and extend from there deep into the thermoclines of the midlatitudes. These anomalies are found in all ocean basins but are most prominently expressed in the Pacific sector of the Southern Ocean. This anomalously low accumulation of anthropogenic CO_2 between 1994 and 2007 corresponds in terms of pattern with the anomalously low air–sea fluxes of CO_2 across most of the Southern Ocean (**Figure 7**). These latter anomalies were computed by subtracting the expected fluxes from the mean fluxes for the 1994–2007 period. For the expected fluxes, we took the average for the periods 1985–1993 and 2008–2016, as these two periods correspond relatively closely to the flux trends without climate variability (cf. **Figure 5**). But quantitatively, the two changes are of rather different magnitudes: The anthropogenic CO_2 storage anomalies in the ocean interior up to 35°S sum up to only approximately 0.2 Pg C (0.5 Pg C up to 45°S), while the integrated air–sea CO_2 flux anomaly over the same period and region amounts to approximately 3 ± 1 Pg C. Thus, the majority of the air–sea CO_2 flux anomaly must be driven by changes in the natural CO_2 fluxes, with the uptake flux of anthropogenic CO_2 enhancing the total flux anomalies. This is in accordance with model-based studies that also emphasized the role of changes in the natural CO_2 fluxes (Le Quéré et al. 2007, Lovenduski et al. 2008). To better understand this conclusion, we first review the proposed drivers and then return to the question of whether the decadal changes are due primarily to changes in the natural or the anthropogenic CO_2 component of the total fluxes.

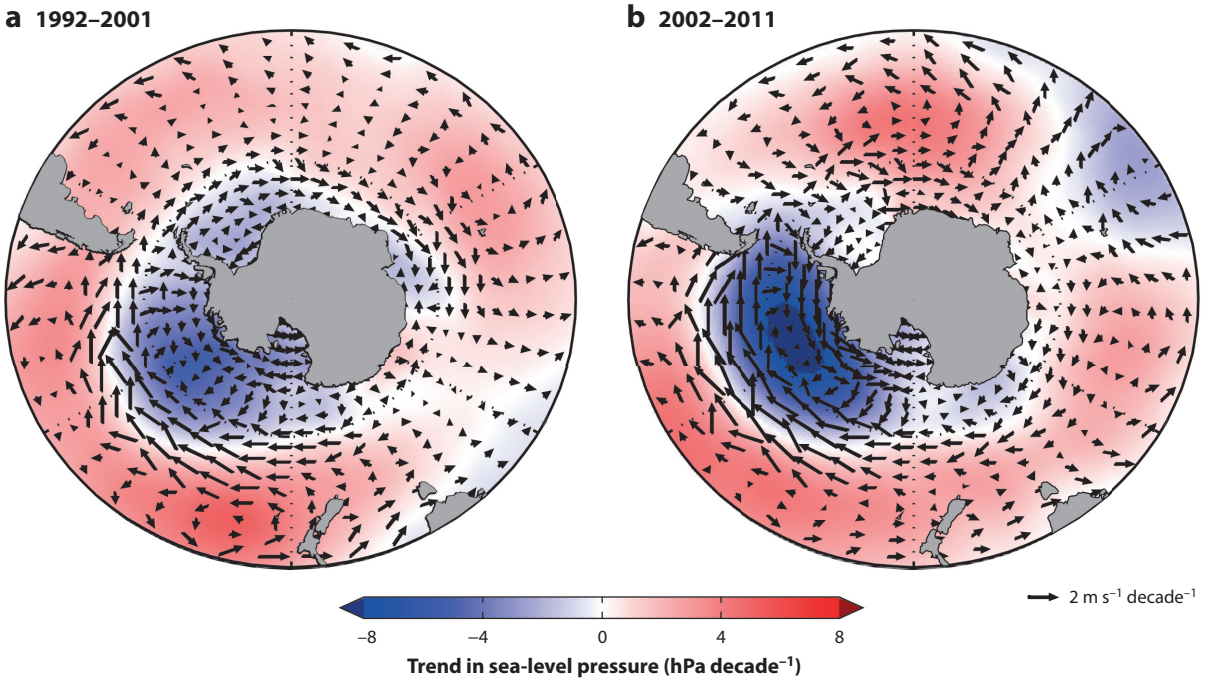

Figure 8

Trends in wind and sea-level pressure. (*a*) Linear trends in wind (*arrows*) and sea-level pressure (*contours*) for 1992–2001. (*b*) The same as panel *a* but for 2002–2011. Figure adapted from Landschützer et al. (2015).

5. MECHANISMS OF DECADAL VARIATIONS

5.1. Drivers

The decadal variations in the fluxes and storage of CO_2 are the result of major reorganizations of the Southern Hemisphere's climate. There is broad consensus that the changes in the 1990s resulted from a southward shift of the main westerly wind belt (**Figure 8**) associated with a trend toward a more positive phase of the Southern Annular Mode (Le Quéré et al. 2007; Lenton & Matear 2007; Lovenduski et al. 2007, 2008). This led to an increased northward Ekman transport at the latitude of the southern Antarctic Circumpolar Current, inducing a stronger upwelling that tends to bring elevated concentrations of DIC to the surface. Since Southern Ocean biology is unable to fully compensate for this increased upwelling, a good fraction of this extra upwelled CO_2 is then lost to the atmosphere, explaining the strong nonthermal trend in the Antarctic zone of the Southern Ocean in **Figure 6*d***.

The mechanisms driving the reinvigoration period are much less clear, particularly since the Southern Annular Mode does not show a change in the trend around 2000 that would indicate a reversal of the wind trends of the 1990s. Instead, a wave number 3 pattern in wind and sea-level pressure developed during the first decade of the 2000, i.e., a pattern that is very reminiscent of the zonal wave 3 (ZW3) pattern identified by Raphael (2004). This pattern manifests itself in a strengthening of the low-pressure field in the Pacific sector off the coast of Antarctica (the Amundsen Sea Low), while in the Atlantic sector, a high-pressure anomaly develops south of Africa. These anomalies are complemented by a low-pressure anomaly in the Indian Ocean sector.

The wind anomalies follow this pattern largely in geostrophic balance—i.e., the zonal winds are strengthened further in the Pacific Ocean sector but tend to weaken in the Atlantic and Indian Ocean sectors. The meridional winds are strengthened with enhanced advection of cold air out of the Antarctic continent over the Ross Sea, while anomalous warm air tends to be advected southward in the Atlantic sector. Thus, overall, while the Southern Ocean in the 1990s experienced a zonally relatively homogeneous trend that was dominated by the southward shift and strengthening of the westerly wind belt, the first decade of the 2000s was characterized by the development of a zonally asymmetric pattern. Some of this asymmetry was already present in the 1990s (e.g., the strengthening trend of the Amundsen Sea Low) but became dominant later.

These zonally asymmetric patterns in the atmosphere also forced the ocean carbon system in a zonally asymmetric manner (**Figure 6*b*,*e*,*f***). In the Pacific sector, the changes in the forcing continued a cooling trend that was already present in the 1990s but was now no longer opposed by a strong positive nonthermal trend. This could be because the cooling was driven primarily by the cold-air advection from the south and/or enhanced freshwater fluxes from an increase in sea-ice advection (Haumann et al. 2016) that led to enhanced stratification, both of which led to a lesser degree of upwelling of the high-DIC waters that tended to overwhelm the cooling trend in the 1990s. In the Atlantic sector, it is primarily the nonthermal trend that drives the trend toward lower pCO_2. Landschützer et al. (2015) suggested that this is likely due to a trend of enhanced stratification from the warming and southward advection of waters from lower latitudes, combined with reduced upwelling. The resulting reduction in surface DIC and possible increase in alkalinity more than overwhelmed the warming-induced increase in pCO_2, explaining the trend toward lower pCO_2.

While the analysis of the trends in the atmospheric drivers permit us to assess the likely set of processes affecting the surface-ocean pCO_2, this is insufficient to determine the processes in the ocean interior. Furthermore, it does not permit us to determine to what degree the changes in the fluxes are driven by natural or anthropogenic CO_2.

5.2. Processes

Through their diagnostic (inverse) modeling framework, DeVries et al. (2017) recently determined the processes driving the changes in ocean carbon uptake and interior ocean redistribution during the last three decades. **Figure 9** summarizes their diagnosed circulation, air–sea fluxes of natural and anthropogenic CO_2, and associated transport for the two decades of the 1990s and the 2000s.

For the 1990s, DeVries et al. (2017) found that there was an anomalously strong meridional overturning circulation in the Southern Ocean, consistent with the southward shift and strengthening of the westerly winds (**Figure 9*a***). They also found that this strong circulation led to an anomalously strong outgassing of natural CO_2, particularly in the region between 55°S and 35°S, coupled with an anomalously low uptake of anthropogenic CO_2. These results explain the weak total uptake, i.e., the sum of natural and anthropogenic CO_2 fluxes, seen in the observation-based analyses (**Figures 5** and **6**). By contrast, the storage rate of anthropogenic CO_2 within the region south of 35°S changes little, implying a weaker northward transport of anthropogenic CO_2 across 35°S.

According to DeVries et al. (2017), the meridional overturning circulation in the first decade of the 2000s slowed considerably (**Figure 9*b***). In particular, they suggested that the net upwelling into the region south of 55°S decreased from 26 sverdrups (Sv) in the 1990s to 18 Sv in the 2000s. They also found that this decreased upwelling led to a strongly reduced outgassing of natural CO_2 and a slight increase in the uptake of anthropogenic CO_2, which explains the observed increase in the total uptake of CO_2 from the atmosphere. As in the 1990s, the storage rates of anthropogenic CO_2 were not much affected.

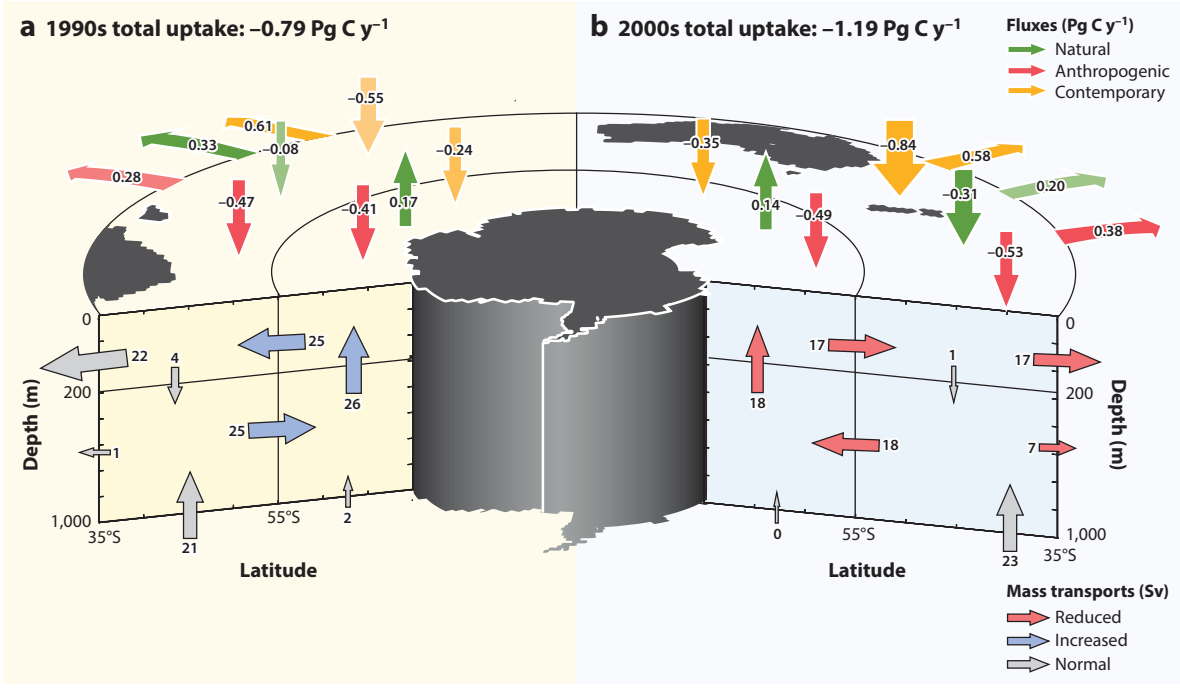

Figure 9

Schematic diagram of the circulation, lateral carbon transports, and air–sea CO_2 fluxes during (*a*) the 1990s and (*b*) the 2000s. Shown in the lower two sections are the mass transports [in sverdrups (Sv)], with the colors indicating significant changes relative to the long-term mean (*red*, reduced transport; *blue*, increased transport; *gray*, not significantly different transport). The vertical arrows on the top surface indicate the air–sea fluxes (in Pg C y^{-1}) for natural CO_2, anthropogenic CO_2, and the sum of the two, i.e., the contemporary CO_2. The sideways arrows depict the lateral transport (in Pg C y^{-1}) of the three components across 35°S. Data are from DeVries et al. (2017).

Taken together, the analyses of DeVries et al. (2017) suggest that the response of the ocean carbon cycle to recent climatic changes in the Southern Ocean has been driven primarily by the ocean circulation, with the changes in the air–sea fluxes of natural and anthropogenic CO_2 reinforcing each other. This confirms our conclusion based on the comparison between the anomalous changes in storage and the anomalous changes in air–sea CO_2 fluxes. But this reinforcement is, in general, a somewhat unusual situation, since in most regions, the anomalous fluxes of natural and anthropogenic CO_2 tend to oppose each other, as is also the case for the mean fluxes in the Southern Ocean south of 55°S (Gruber et al. 2009) (**Figures 2** and **9**). This difference could be explained by the observation of a relatively short residence time of the surface waters in the northward-flowing branch of the Southern Ocean's meridional overturning circulation, i.e., the upper cell. As this transport accelerates, the reduction in the residence time could reduce the uptake of anthropogenic CO_2 in this region, as the waters are no longer in touch with the atmosphere for the roughly 10 months necessary to equilibrate with the atmospheric perturbation (Broecker & Peng 1974, Sarmiento & Gruber 2006). This effect was not seen in ocean models (e.g., Lovenduski et al. 2008), perhaps because these coarse-resolution models have formation regions that are too broad for mode and intermediate waters (Lachkar et al. 2009).

While the analyses of DeVries et al. (2017) are highly consistent with the trends in the surface CO_2 fluxes, their ocean-interior changes only partially explain the negative anomalies seen in the accumulation of anthropogenic CO_2 (Gruber et al. 2018) (**Figure 7**). This is likely to some

degree a consequence of the different time periods being investigated, with DeVries et al. (2017) analyzing the 1990s versus the 2000s, while Gruber et al. (2018) analyzed the integrated changes between 1994 and 2007. The reduction in storage seen by Gruber et al. (2018) may contradict, at first sight, the increase in the storage of the CFCs in the mode waters over roughly the same time period (1991 through 2005) (Waugh et al. 2013). One possibility to reconcile this is by again comparing the air–sea gas exchange equilibration timescale with the surface residence time. While the surface residence time is the same for both gases, the equilibration time for the air–sea gas exchange of anthropogenic CO_2 (10 months) is 10 times that for CFCs (~1 month). Thus, even though the speedup of the overturning circulation reduced the surface residence considerably, it remained longer than the equilibration time for the air–sea gas exchange of CFCs. This resulted in a considerable increase in the uptake and accumulation of CFCs in the mode waters. The opposite probably occurred for anthropogenic CO_2, since the surface residence time presumably decreased below the equilibration timescale.

The diagnosed dominance of circulation in generating the strong decadal variations in the Southern Ocean carbon sink also suggests that ocean biology has played a relatively minor role. Landschützer et al. (2015) investigated the possible presence of trends in ocean chlorophyll as seen by satellites but could not detect any significant changes during the 1998–2011 period. This limited role of ocean biology is also supported by its relatively weak and overall inhomogeneous response to interannual changes in the Southern Annular Mode (Lovenduski & Gruber 2005). By contrast, Gregor et al. (2018) found a strong link between variations in pCO_2 and those of chlorophyll over a similar time period, but this link was present only in summer months, i.e., when ocean biology dominates the pCO_2 variability (see also **Figure 4**).

6. DISCUSSION

6.1. Local Versus Remote Forcing

Although the main processes controlling the variability of the Southern Ocean carbon sink are well established, it remains a fascinating and largely unresolved puzzle how the interaction of these processes, none of which varies strongly on decadal timescales, can generate such a dominant decadal variability signal in this sink. Similar but smaller-amplitude decadal variations in the air–sea CO_2 fluxes are present in the North Atlantic and North Pacific (Pérez et al. 2013, Landschützer et al. 2016). While this could be coincidence, it could also indicate the presence of a joint driver, most likely located in the tropics.

The tropics are well known to influence climate variations in the high latitudes, mainly through atmospheric teleconnections that alter weather and climate in the higher latitudes through stationary waves induced by changes in tropical convection (Karoly 1989). In the Southern Hemisphere, such teleconnection patterns are well known for the Pacific sector [e.g., the Pacific–South American mode (Mo & Higgins 1998)], influencing sea-level pressure, winds, sea-surface temperature, and sea-ice extent in and around the Southern Ocean (e.g., Fogt & Bromwich 2006, Cerrone et al. 2017). Although the strongest changes associated with remote forcing from the tropical Pacific are in the Pacific sector, these signals also extend into the Atlantic and Indian Ocean sectors (Ferster et al. 2018). Cerrone et al. (2017) recently demonstrated how this remote forcing interacts with the high-latitude modes of variability, namely the Southern Annular Mode and the ZW3 pattern (Raphael 2004), generating a distinct pattern of variability. The focus of much recent research has been on sea-ice variations and the cooling trend in the Pacific sector. The role of such interactions has not yet been explored with regard to the variations of the air–sea CO_2 fluxes. But it is conceivable that such interactions are at the heart of how the interannual- to decadal-timescale signals

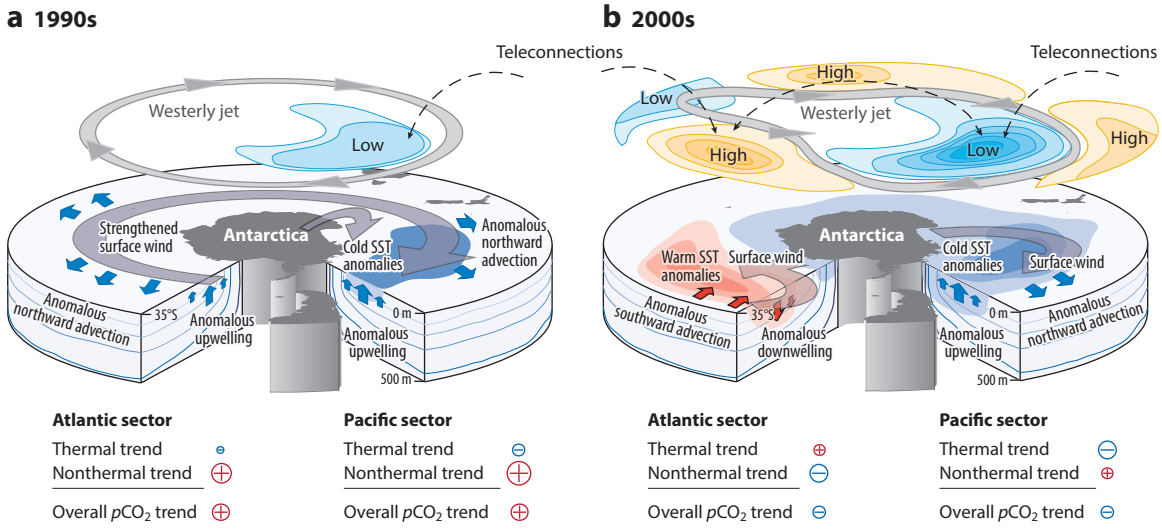

Figure 10

Conceptual diagram of the processes driving the changes in the Southern Ocean carbon fluxes, contrasting (*a*) the situation in the 1990s with (*b*) the situation in the 2000s. Shown are the changes in the atmospheric forcing, the responses in sea-surface temperature (SST) and upper-ocean circulation, and the resulting impacts on the surface-ocean pCO_2 trends, split into their thermal and nonthermal components for the Atlantic and Pacific sectors. Figure adapted and expanded from Landschützer et al. (2015).

present in the tropics can rectify the local, typically higher-frequency processes in the Southern Ocean to generate the lower-frequency (decadal) variations. The interaction of the decadal variations of the El Niño–Southern Oscillation with the Southern Annular Mode and the ZW3 pattern is likely of particular importance, because the trends in the 1990s had a strong Southern Annular Mode signature, while the trends in the 2000s had a strong ZW3 signature (**Figure 10**). A possible scenario is that the Southern Annular Mode was particularly strong during the 1990s, a decade dominated by the El Niño–Southern Oscillation, while the ZW3 mode was strong during the La Niña–dominated decade of the 2000s. This scenario is consistent with the ZW3 mode having undergone a very rapid mode shift around 2000 (S. Schemm, personal communication).

While the role of such teleconnections is not well established, there exists broad consensus that the decadal-timescale signal in the air–sea CO_2 fluxes results primarily from atmospheric forcing altering ocean circulation, sea-surface temperature, and stratification. **Figure 10** summarizes the different drivers and processes during the 1990s and the first decade of the twenty-first century.

The long-term trend toward an increasing Southern Ocean carbon sink is highly likely to be attributable to the increase in atmospheric CO_2. The strong variations around this long-term mean trend were determined to be driven primarily by natural CO_2, perhaps enhanced by variations in the uptake flux of anthropogenic CO_2. But whether the atmospheric and oceanic drivers causing these variations are a consequence of natural (unforced) climate variability or a manifestation of a human-induced climatic change has not been systematically analyzed. While the long-term trend toward a more positive Southern Annular Mode is driven partially by human-induced changes [a reduction in ozone and increase in atmospheric CO_2 (Gillett & Thompson 2003)], the other modes of variability in the Southern Hemisphere have so far shown no discernible impact of anthropogenic climate change. Thus, it is more likely than not that the strong decadal variations in the Southern Ocean carbon sink are a result of unforced (natural) variability (see also Li & Ilyina 2018).

6.2. Future Evolution and Predictability

The strong role of atmospheric forcing and ocean circulation in generating decadal variations in air–sea CO_2 fluxes suggests that there is some short-term predictability in the Southern Ocean carbon sink. But experiments with a large ensemble of simulations started from the same point in time, but with small initial perturbations, show that the modeled CO_2 fluxes of the different ensemble members drift apart very quickly (N.S. Lovenduski, S.G. Yeager, K. Lindsay & M.C. Long, manuscript in preparation) (**Figure 11*a–c***). In terms of the level of correlation between the actual and forecast magnitudes of the air–sea CO_2 flux, the system loses predictability within a few years. While there is still some skill in a perfect model system (i.e., no initialization error),

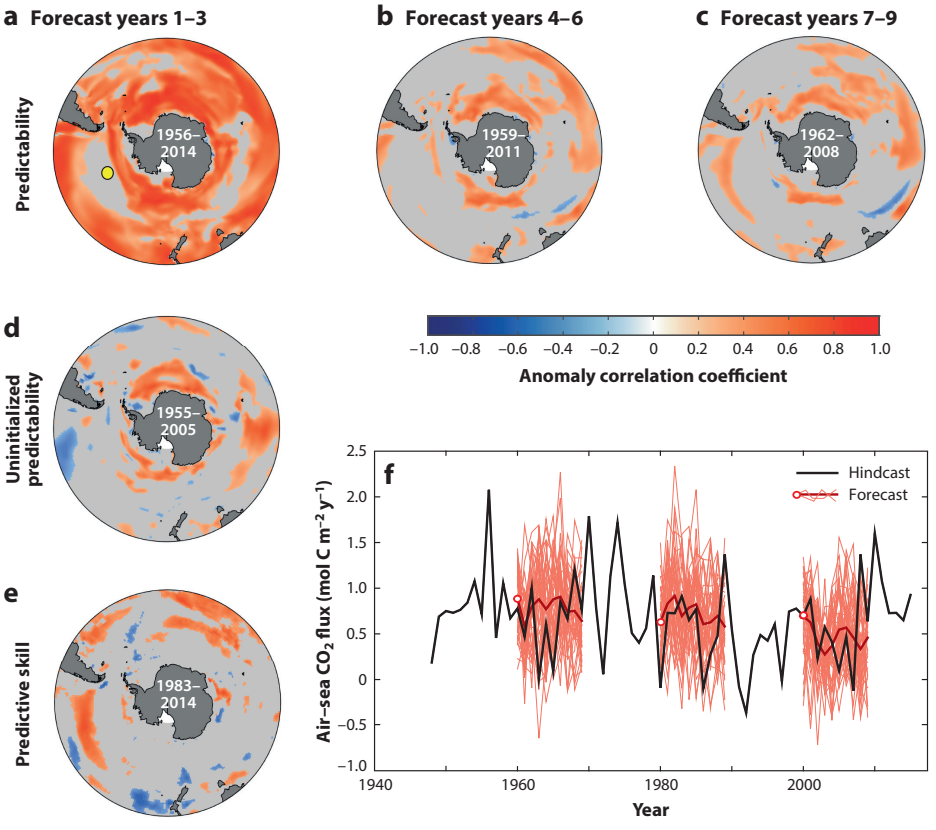

Figure 11

The predictability of the Southern Ocean carbon sink. (*a–e*) Maps of anomaly correlation coefficients of the annual-mean air–sea CO_2 flux from the Community Earth System Model–Decadal Prediction system relative to the forced ocean–sea-ice hindcast simulation used for initialization for forecast lead times of 1–3 years, 4–6 years, and 7–9 years (panels *a–c*, respectively); the uninitialized Community Earth System Model–Large Ensemble system (panel *d*); and the self-organizing map–feed-forward neural network (SOM-FFN) observational product (Landschützer et al. 2015) (panel *e*). (*f*) Annual-mean air–sea CO_2 flux at a location in the South Pacific (*yellow dot* in panel *a*) from the forced ocean–sea-ice hindcast (*black line*) and a 40-member decadal forecast ensemble (*red lines*, with the *thick red line* indicating the ensemble mean) for forecasts initiated in 1960, 1980, and 2000 (forecasts initiated in other years have been omitted for visual clarity). The forecasts have been corrected for model drift. The decadal prediction simulations and drift-correction procedure have been described by Yeager et al. (2018). Figure adapted from N.S. Lovenduski, S.G. Yeager, K. Lindsay & M.C. Long (manuscript in preparation).

in the first three years the skill is essentially lost. The only exceptions are the ice-covered regions and the subtropics. While the higher predictability in the subtropics is likely associated with longer persistence, the higher predictability in the sea-ice-covered regions is not engendered by the initialization. Rather, this predictability emerges from the ensemble members staying tightly together in this region—i.e., a high skill is achieved even when the model is initialized with a random state (**Figure 11*d***). The low predictability of the Southern Ocean contrasts with the substantially longer prediction timescale in other regions in the global ocean (Li et al. 2016, Séférian et al. 2018).

Beyond a few years into the future, the dominant mode of variability in the Southern Ocean carbon sink will remain the internal (unforced) mode of variability until approximately 2050, and only then will the emission scenario become the dominant source of uncertainty (Lovenduski et al. 2016). Current-generation Earth system models tend to estimate different trajectories for the future ocean carbon sink (e.g., Hauck et al. 2015), although Kessler & Tjiputra (2016) also demonstrated that the contemporary Southern Ocean carbon uptake can be used as an emergent constraint for future uptake up to 2100. Even larger changes may be in store if the simulations are extended to 2300 in a high-CO_2-emission scenario. Moore et al. (2018) demonstrated a large redistribution of primary production [and consequently also air–sea CO_2 fluxes (Hauck et al. 2015)] in an extended run, with a large increase in the productivity in the high latitudes of the Southern Ocean, while much of the rest of the ocean was simulated to experience a drastic decrease. This was determined to be the result of a strong nutrient trapping in the Southern Ocean in this high-CO_2 world (see also Laufkötter & Gruber 2018).

SUMMARY POINTS

1. The Southern Ocean sink for atmospheric CO_2 varies on all timescales, with the seasonal and decadal variations standing out. The former is driven primarily by strongly compensating effects of ocean biology, mixing, and warming/cooling.
2. The decadal variability of the ocean carbon sink results primarily from atmospheric variations inducing changes in ocean circulation, sea-surface temperature, and stratification. The large-scale zonal coherency of the response of the ocean carbon cycle is a result of different processes acting in the different ocean basins, particularly during the strengthening period after the year 2000. Atmospheric teleconnections might play an important but poorly constrained role in generating the strong decadal signature of the Southern Ocean carbon sink.
3. The large changes in the surface fluxes leave a detectable imprint in the ocean-interior accumulation of anthropogenic CO_2, which suggests that both natural and anthropogenic CO_2 fluxes are affected by decadal variations.
4. Models poorly represent the decadal variations of the Southern Ocean carbon sink. In addition, their skill at making decadal predictions in this area is low.

FUTURE ISSUES

1. The complex time-evolving nature of the Southern Ocean carbon sink makes the continuation and expansion of observational efforts a necessity. The emerging opportunity to use Argo floats equipped with biogeochemical sensors needs to be further explored,

particularly since they provide, for the first time, winter observations in many parts of the Southern Ocean.

2. Ocean biogeochemical models need to take a substantial step forward in their ability to simulate the Southern Ocean carbon sink. The seasonal cycle can serve as an important benchmark.
3. While a first attempt was made here to connect the surface changes with those occurring in the ocean interior, this area needs to be further developed, particularly with regard to the processes driving these changes. Doing so will require a better identification of the changes in storage of natural CO_2.
4. We need a better understanding of the Southern Ocean as a coupled ocean–atmosphere–sea-ice system.

DISCLOSURE STATEMENT

The authors are not aware of any affiliations, memberships, funding, or financial holdings that might be perceived as affecting the objectivity of this review.

ACKNOWLEDGMENTS

We are grateful to the large number of scientists and institutions that support the collection of surface and interior ocean carbon observations in the Southern Ocean. Without their dedication and long-term commitments, almost none of the insights presented here would exist. We also acknowledge the groups that assembled these data, subjected them to secondary quality control, and provided the community with open, easy-to-use data sets. Specifically, we would like to name the Surface Ocean CO_2 Atlas (SOCAT) team under the leadership of D. Bakker and the Global Ocean Data Analysis Project (GLODAP) team under the leadership of A. Olsen. We also thank C. Le Quéré and coauthors for providing access to the hindcast model output from their 2017 global carbon budget. The work of N.G. was funded by ETH Zurich, with additional support from the Swiss National Science Foundation (Project SOGate). N.S.L. is grateful for funding from the National Science Foundation (OCE-1752724, OCE-1558225, and PLR-1543457). Community Earth System Model computing resources were provided by the National Energy Research Scientific Computing Center of the US Department of Energy and by the Cheyenne supercomputer at the Computational and Information Systems Lab sponsored by the National Science Foundation. P.L.'s work was funded by the Max Planck Society.

LITERATURE CITED

Anav A, Friedlingstein P, Kidston M, Bopp L, Ciais P, et al. 2013. Evaluating the land and ocean components of the global carbon cycle in the CMIP5 Earth system models. *J. Clim.* 26:6801–43

Bakker DCE, Pfeil B, Landa CS, Metzl N, O'Brien KM, et al. 2016. A multi-decade record of high-quality CO_2 data in version 3 of the Surface Ocean CO_2 Atlas (SOCAT). *Earth Syst. Sci. Data* 8:383–413

Bakker DCE, Pfeil B, Landa CS, Metzl N, O'Brien KM, et al. 2017. *Surface Ocean CO_2 Atlas Database Version 5 (SOCATv5) (NCEI accession 0163180)*. Data Set Version 2.2, Natl. Cent. Environ. Inf., Natl. Ocean. Atmos. Adm., Silver Spring, MD. **https://data.nodc.noaa.gov/cgi-bin/iso?id=gov.noaa.nodc:0163180**

Bopp L, Lévy M, Resplandy L, Sallée JB. 2015. Pathways of anthropogenic carbon subduction in the global ocean. *Geophys. Res. Lett.* 42:6416–23

Boyd PW, Watson AJ, Law CS, Abraham ER, Trull T, et al. 2000. A mesoscale phytoplankton bloom in the polar Southern Ocean stimulated by iron fertilization. *Nature* 407:695–702

Broecker WS, Peng TH. 1974. Gas exchange rates between air and sea. *Tellus* 26:21–35

Buitenhuis ET, Rivkin RB, Séailley S, Le Quéré C. 2010. Biogeochemical fluxes through microzooplankton. *Glob. Biogeochem. Cycles* 24:GB4015

Butterworth BJ, Miller SD. 2016. Air-sea exchange of carbon dioxide in the Southern Ocean and Antarctic marginal ice zone. *Geophys. Res. Lett.* 43:7223–30

Caldeira K, Duffy PB. 2000. The role of the Southern Ocean in uptake and storage of anthropogenic carbon dioxide. *Science* 287:620–22

Carter BR, Feely RA, Mecking S, Cross JN, Macdonald AM, et al. 2017. Two decades of Pacific anthropogenic carbon storage and ocean acidification along Global Ocean Ship-based Hydrographic Investigations Program sections P16 and P02. *Glob. Biogeochem. Cycles* 31:306–27

Cerrone D, Fusco G, Simmonds I, Aulicino G, Budillon G. 2017. Dominant covarying climate signals in the Southern Ocean and Antarctic sea ice influence during the last three decades. *J. Clim.* 30:3055–72

Clement D, Gruber N. 2018. The eMLR(C*) method to determine decadal changes in the global ocean storage of anthropogenic CO_2. *Glob. Biogeochem. Cycles.* 32:654–79

DeVries T. 2014. The oceanic anthropogenic CO_2 sink: storage, air-sea fluxes, and transports over the industrial era. *Glob. Biogeochem. Cycles* 28:631–47

DeVries T, Holzer M, Primeau F. 2017. Recent increase in oceanic carbon uptake driven by weaker upper-ocean overturning. *Nature* 542:215–18

Doney SC, Lima I, Feely RA, Glover DM, Lindsay K, et al. 2009. Mechanisms governing interannual variability in upper-ocean inorganic carbon system and air–sea CO_2 fluxes: physical climate and atmospheric dust. *Deep-Sea Res. II* 56:640–55

Fay AR, McKinley GA. 2013. Global trends in surface ocean pCO_2 from in situ data. *Glob. Biogeochem. Cycles* 27:541–57

Fay AR, McKinley GA, Lovenduski NS. 2014. Southern Ocean carbon trends: sensitivity to methods. *Geophys. Res. Lett.* 41:6833–40

Ferster BS, Subrahmanyam B, Macdonald AM. 2018. Confirmation of ENSO-Southern Ocean teleconnections using satellite-derived SST. *Remote Sens.* 10:331

Fogt RL, Bromwich DH. 2006. Decadal variability of the ENSO teleconnection to the high latitude South Pacific governed by coupling with the Southern Annular Mode. *J. Clim.* 19:979–97

Friis K, Körtzinger A, Pätsch J, Wallace DWR. 2005. On the temporal increase of anthropogenic CO_2 in the subpolar North Atlantic. *Deep-Sea Res. I* 52:681–98

Frölicher TL, Sarmiento JL, Paynter DJ, Dunne JP, Krasting JP, Winton M. 2015. Dominance of the Southern Ocean in anthropogenic carbon and heat uptake in CMIP5 models. *J. Clim.* 28:862–86

Gammon RH, Cline J, Wisegarver D. 1982. Chlorofluoromethanes in the northeast Pacific Ocean: measured vertical distributions and application as transient tracers of upper ocean mixing. *J. Geophys. Res.* 87:9441–54

Gillett NP, Thompson DWJ. 2003. Simulation of recent southern hemisphere climate change. *Science* 302:273–75

Gloor M, Gruber N, Sarmiento JL, Sabine CL, Feely RA, Roedenbeck C. 2003. A first estimate of present and pre-industrial air-sea CO_2 flux patterns based on ocean interior carbon measurements and models. *Geophys. Res. Lett.* 30:10-1–4

GO-SHIP (Glob. Ocean Ship-Based Hydrogr. Investig. Program). 2017. GO-SHIP reference sections. *GO-SHIP*. **http://www.go-ship.org/RefSecs/goship_ref_secs.html**

Graven HD, Gruber N, Key R, Khatiwala S, Giraud X. 2012. Changing controls on oceanic radiocarbon: new insights on shallow-to-deep ocean exchange and anthropogenic CO_2 uptake. *J. Geophys. Res.* 117:C10005

Gray AR, Johnson KS, Bushinsky SM, Riser SC, Russell JL, et al. 2018. Autonomous biogeochemical floats detect significant carbon dioxide outgassing in the high-latitude Southern Ocean. *Geophys. Res. Lett.* 45:9049–57

Gregor L, Kok S, Monteiro PMS. 2018. Interannual drivers of the seasonal cycle of CO_2 in the Southern Ocean. *Biogeosciences* 15:2361–78

Gruber N. 1998. Anthropogenic CO_2 in the Atlantic Ocean. *Glob. Biogeochem. Cycles* 12:165–91
Gruber N, Clement D, Feely RA, van Heuven S, Hoppema M, et al. 2018. The oceanic sink for anthropogenic CO_2 since the mid-1990s. *Science*. In review
Gruber N, Doney SC. 2009. Ocean biogeochemistry and ecology, modeling of. In *Encyclopedia of Ocean Sciences*, Vol. 2, ed. JH Steele, KK Turekian, SA Thorpe, pp. 89–104. San Diego, CA: Academic. 2nd ed.
Gruber N, Gloor M, Mikaloff Fletcher SE, Doney SC, Dutkiewicz S, et al. 2009. Oceanic sources, sinks, and transport of atmospheric CO_2. *Glob. Biogeochem. Cycles* 23:GB1005
Gruber N, Sarmiento JL. 2002. Large-scale biogeochemical/physical interactions in elemental cycles. In *The Sea*, Vol. 12: *Biological-Physical Interactions in the Oceans*, ed. AR Robinson, JJ McCarthy, BJ Rothschild, pp. 337–99. New York: Wiley & Sons
Gruber N, Sarmiento JL, Stocker TF. 1996. An improved method for detecting anthropogenic CO_2 in the oceans. *Glob. Biogeochem. Cycles* 10:809–37
Hauck J, Köhler P, Wolf-Gladrow D, Völker C. 2016. Iron fertilisation and century-scale effects of open ocean dissolution of olivine in a simulated CO_2 removal experiment. *Environ. Res. Lett.* 11:24007
Hauck J, Völker C, Wolf-Gladrow DA, Laufkötter C, Vogt M, et al. 2015. On the Southern Ocean CO_2 uptake and the role of the biological carbon pump in the 21st century. *Glob. Biogeochem. Cycles* 29:1451–70
Haumann FA, Gruber N, Münnich M, Frenger I, Kern S. 2016. Sea-ice transport driving Southern Ocean salinity and its recent trends. *Nature* 537:89–92
Hoppema M, Roether W, Bellerby RGJ, de Baar HJW. 2001. Direct measurements reveal insignificant storage of anthropogenic CO_2 in the Abyssal Weddell Sea. *Geophys. Res. Lett.* 28:1747–50
Ilyina T, Six KD, Segschneider J, Maier-Reimer E, Li H, Núñez-Riboni I. 2013. Global ocean biogeochemistry model HAMOCC: model architecture and performance as component of the MPI-Earth system model in different CMIP5 experimental realizations. *J. Adv. Model. Earth Syst.* 5:287–315
Ito T, Woloszyn M, Mazloff M. 2010. Anthropogenic carbon dioxide transport in the Southern Ocean driven by Ekman flow. *Nature* 463:80–83
Iudicone D, Rodgers KB, Plancherel Y, Aumont O, Ito T, et al. 2016. The formation of the ocean's anthropogenic carbon reservoir. *Sci. Rep.* 6:35473
Jiang C, Gille ST, Sprintall J, Sweeney C. 2014. Drake passage oceanic pCO_2: evaluating CMIP5 coupled carbon–climate models using in situ observations. *J. Clim.* 27:76–100
Johnson GC, Bryden HL. 1989. On the size of the Antarctic Circumpolar Current. *Deep-Sea Res. A* 36:39–53
Karoly DJ. 1989. Southern Hemisphere circulation features associated with El Niño-Southern Oscillation events. *J. Clim.* 2:1239–52
Kay JE, Deser C, Phillips A, Mai A, Hannay C, et al. 2015. The Community Earth System Model (CESM) large ensemble project: a community resource for studying climate change in the presence of internal climate variability. *Bull. Am. Meteorol. Soc.* 96:1333–49
Kessler A, Tjiputra J. 2016. The Southern Ocean as a constraint to reduce uncertainty in future ocean carbon sinks. *Earth Syst. Dyn.* 7:295–312
Key RM, Kozyr A, Sabine CL, Lee K, Wanninkhof R, et al. 2004. A global ocean carbon climatology: results from Global Data Analysis Project (GLODAP). *Glob. Biogeochem. Cycles* 18:GB4031
Khatiwala S, Primeau F, Hall T. 2009. Reconstruction of the history of anthropogenic CO_2 concentrations in the ocean. *Nature* 462:346–49
Khatiwala S, Tanhua T, Mikaloff Fletcher SE, Gerber M, Doney SC, et al. 2013. Global ocean storage of anthropogenic carbon. *Biogeosciences* 10:2169–91
Kouketsu S, Murata A. 2014. Detecting decadal scale increases in anthropogenic CO_2 in the ocean. *Geophys. Res. Lett.* 41:4594–600
Lachkar Z, Orr JC, Dutay JC. 2009. Seasonal and mesoscale variability of oceanic transport of anthropogenic CO_2. *Biogeosciences* 6:2509–23
Landschützer P, Gruber N, Bakker DCE. 2016. Decadal variations and trends of the global ocean carbon sink. *Glob. Biogeochem. Cycles* 30:1396–417
Landschützer P, Gruber N, Bakker DCE, Schuster U, Nakaoka S, et al. 2013. A neural network-based estimate of the seasonal to inter-annual variability of the Atlantic Ocean carbon sink. *Biogeosciences* 10:7793–815
Landschützer P, Gruber N, Bakker DCE, Stemmler I, Six KD. 2018. Strengthening seasonal marine CO_2 variations due to increasing atmospheric CO_2. *Nat. Clim. Change* 8:146–50

Landschützer P, Gruber N, Haumann FA, Rödenbeck C, Bakker DCE, et al. 2015. The reinvigoration of the Southern Ocean carbon sink? *Science* 349:1221–24
Laufkötter C, Gruber N. 2018. Will marine productivity wane? *Science* 359:1103–4
Law RM, Ziehn T, Matear RJ, Lenton A, Chamberlain MA, et al. 2017. The carbon cycle in the Australian Community Climate and Earth System Simulator (ACCESS-ESM1) – part 1: model description and pre-industrial simulation. *Geosci. Model Dev.* 10:2567–90
Le Quéré C, Andrew RM, Friedlingstein P, Sitch S, Pongratz J, et al. 2018. Global carbon budget 2017. *Earth Syst. Sci. Data* 10:405–48
Le Quéré C, Rodenbeck C, Buitenhuis ET, Conway TJ, Langenfelds R, et al. 2007. Saturation of the Southern Ocean CO_2 sink due to recent climate change. *Science* 316:1735–38
Lee K, Choi SD, Park GH, Wanninkhof R, Peng TH, et al. 2003. An updated anthropogenic CO_2 inventory in the Atlantic Ocean. *Glob. Biogeochem. Cycles* 17:1116
Lenton A, Matear RJ. 2007. Role of the Southern Annular Mode (SAM) in Southern Ocean CO_2 uptake. *Glob. Biogeochem. Cycles* 21:GB2016
Lenton A, Tilbrook B, Law RM, Bakker D, Doney SC, et al. 2013. Sea–air CO_2 fluxes in the Southern Ocean for the period 1990–2009. *Biogeosciences* 10:4037–54
Li H, Ilyina T. 2018. Current and future decadal trends in the oceanic carbon uptake are dominated by internal variability. *Geophys. Res. Lett.* 45:916–25
Li H, Ilyina T, Müller WA, Sienz F. 2016. Decadal predictions of the North Atlantic CO_2 uptake. *Nat. Commun.* 7:11076
Lovenduski NS, Gruber N. 2005. Impact of the Southern Annular Mode on Southern Ocean circulation and biology. *Geophys. Res. Lett.* 32:L11603
Lovenduski NS, Gruber N, Doney SC. 2008. Toward a mechanistic understanding of the decadal trends in the Southern Ocean carbon sink. *Glob. Biogeochem. Cycles* 22:GB3016
Lovenduski NS, Gruber N, Doney SC, Lima ID. 2007. Enhanced CO_2 outgassing in the Southern Ocean from a positive phase of the Southern Annular Mode. *Glob. Biogeochem. Cycles* 21:GB2026
Lovenduski NS, Ito T. 2009. The future evolution of the Southern Ocean CO_2 sink. *J. Mar. Res.* 67:597–617
Lovenduski NS, McKinley GA, Fay AR, Lindsay K, Long MC. 2016. Partitioning uncertainty in ocean carbon uptake projections: internal variability, emission scenario, and model structure. *Glob. Biogeochem. Cycles* 30:1276–87
Majkut JD, Carter BR, Frolicher TL, Dufour CO, Rodgers KB, Sarmiento JL. 2014. An observing system simulation for Southern Ocean carbon dioxide uptake. *Philos. Trans. R. Soc. A* 372:20130046
Marshall J, Speer K. 2012. Closure of the meridional overturning circulation through Southern Ocean upwelling. *Nat. Geosci.* 5:171–80
Matsumoto K, Gruber N. 2005. How accurate is the estimation of anthropogenic carbon in the ocean? An evaluation of the ΔC^* method. *Glob. Biogeochem. Cycles* 19:GB3014
Matsumoto K, Sarmiento JL, Brzezinski MA. 2002. Silicic acid leakage from the Southern Ocean as possible mechanism for explaining glacial atmospheric pCO_2. *Glob. Biogeochem. Cycles* 16:5-1–23
McElroy MB. 1983. Marine biological controls on atmospheric CO_2 and climate. *Nature* 302:328–29
McKinley GA, Fay AR, Lovenduski NS, Pilcher DJ. 2017. Natural variability and anthropogenic trends in the ocean carbon sink. *Annu. Rev. Mar. Sci.* 9:125–50
McKinley GA, Pilcher DJ, Fay AR, Lindsay K, Long MC, Lovenduski NS. 2016. Timescales for detection of trends in the ocean carbon sink. *Nature* 530:469–72
McNeil BI, Matear RJ. 2013. The non-steady state oceanic CO_2 signal: its importance, magnitude and a novel way to detect it. *Biogeosciences* 10:2219–28
McNeil BI, Tilbrook B, Matear RJ. 2001. Accumulation and uptake of anthropogenic CO_2 in the Southern Ocean, south of Australia from 1968 to 1996. *J. Geophys. Res.* 106:31431–45
Mikaloff Fletcher SE. 2015. An increasing carbon sink? *Science* 349:1165
Mikaloff Fletcher SE, Gruber N, Jacobson AR, Doney SC, Dutkiewicz S, et al. 2006. Inverse estimates of anthropogenic CO_2 uptake, transport, and storage by the ocean. *Glob. Biogeochem. Cycles* 20:GB2002
Mikaloff Fletcher SE, Gruber N, Jacobson AR, Gloor M, Doney SC, et al. 2007. Inverse estimates of the oceanic sources and sinks of natural CO_2 and the implied oceanic carbon transport. *Glob. Biogeochem. Cycles* 21:GB1010

Miller RL, Schmidt GA, Shindell DT. 2006. Forced annular variations in the 20th century Intergovernmental Panel on Climate Change Fourth Assessment Report models. *J. Geophys. Res. Atmos.* 111:D18101

Mo KC, Higgins RW. 1998. The Pacific–South American modes and tropical convection during the Southern Hemisphere winter. *Mon. Weath. Rev.* 126:1581–96

Mongwe NP, Vichi M, Monteiro PMS. 2018. The seasonal cycle of pCO_2 and CO_2 fluxes in the Southern Ocean: diagnosing anomalies in CMIP5 Earth system models. *Biogeosciences* 155:2851–72

Moore JK, Fu W, Primeau F, Britten GL, Lindsay K, et al. 2018. Sustained climate warming drives declining marine biological productivity. *Science* 359:1139–43

Morrison AK, Frölicher TL, Sarmiento JL. 2015. Upwelling in the Southern Ocean. *Phys. Today* 68:27–32

Munk WH, Palmén E. 1951. Note on the dynamics of the Antarctic Circumpolar Current. *Tellus* 3:53–55

Munro DR, Lovenduski NS, Takahashi T, Stephens BB, Newberger T, Sweeney C. 2015. Recent evidence for a strengthening CO_2 sink in the Southern Ocean from carbonate system measurements in the Drake Passage (2002–2015). *Geophys. Res. Lett.* 42:7623–30

Olsen A, Key RM, van Heuven S, Lauvset SK, Velo A, et al. 2016. The Global Ocean Data Analysis Project version 2 (GLODAPv2): an internally consistent data product for the world ocean. *Earth Syst. Sci. Data* 8:297–323

Orr JC, Maier-Reimer E, Mikolajewicz U, Monfray P, Sarmiento JL, et al. 2001. Global oceanic uptake of anthropogenic carbon dioxide as predicted by four 3-D ocean models. *Glob. Biogeochem. Cycles* 15:43–60

Pérez FF, Mercier H, Vázquez-Rodríguez M, Lherminier P, Velo A, et al. 2013. Atlantic Ocean CO_2 uptake reduced by weakening of the meridional overturning circulation. *Nat. Geosci.* 6:146–52

Raphael MN. 2004. A zonal wave 3 index for the Southern Hemisphere. *Geophys. Res. Lett.* 31:L23212

Ritter R, Landschützer P, Gruber N, Fay AR, Iida Y, et al. 2017. Observation-based trends of the Southern Ocean carbon sink. *Geophys. Res. Lett.* 44:12339–48

Rödenbeck C, Bakker DCE, Gruber N, Iida Y, Jacobson AR, et al. 2015. Data-based estimates of the ocean carbon sink variability – first results of the Surface Ocean pCO_2 Mapping intercomparison (SOCOM). *Biogeosciences* 12:7251–78

Rödenbeck C, Bakker DCE, Metzl N, Olsen A, Sabine C, et al. 2014. Interannual sea–air CO_2 flux variability from an observation-driven ocean mixed-layer scheme. *Biogeosciences* 11:4599–613

Sabine CL, Feely RA, Gruber N, Key RF, Lee K, et al. 2004. The oceanic sink for anthropogenic CO_2. *Science* 305:367–71

Sabine CL, Tanhua T. 2010. Estimation of anthropogenic CO_2 inventories in the ocean. *Annu. Rev. Mar. Sci.* 2:175–98

Sallée JB, Matear RJ, Rintoul SR, Lenton A. 2012. Localized subduction of anthropogenic carbon dioxide in the Southern Hemisphere oceans. *Nat. Geosci.* 5:579–84

Sarmiento JL, Gruber N. 2006. *Ocean Biogeochemical Dynamics*. Princeton, NJ: Princeton Univ. Press

Sarmiento JL, Gruber N, Brzezinski MA, Dunne JP. 2004. High-latitude controls of thermocline nutrients and low-latitude biological productivity. *Nature* 427:56–60

Sarmiento JL, Hughes TMC, Stouffer RJ, Manabe S. 1998. Simulated response of the ocean carbon cycle to anthropogenic climate warming. *Nature* 393:245–49

Sarmiento JL, Toggweiler JR. 1984. A new model for the role of the oceans in determining atmospheric pCO_2. *Nature* 308:621–24

Schwinger J, Goris N, Tjiputra JF, Kriest I, Bentsen M, et al. 2016. Evaluation of NorESM-OC (versions 1 and 1.2), the ocean carbon-cycle stand-alone configuration of the Norwegian Earth System Model (NorESM1). *Geosci. Model Dev.* 9:2589–622

Séférian R, Berthet S, Chevallier M. 2018. Assessing the decadal predictability of land and ocean carbon uptake. *Geophys. Res. Lett.* 45:2455–66

Séférian R, Bopp L, Gehlen M, Orr JC, Ethé C, et al. 2013. Skill assessment of three earth system models with common marine biogeochemistry. *Clim. Dyn.* 40:2549–73

Siegenthaler U, Wenk T. 1984. Rapid atmospheric CO_2 variations and ocean circulation. *Nature* 308:624–26

Takahashi T, Olafsson J, Goddard JG, Chipman DW, Sutherland SC. 1993. Seasonal variation of CO_2 and nutrients in the high-latitude surface oceans: a comparative study. *Glob. Biogeochem. Cycles* 7:843–78

Takahashi T, Sutherland SC, Wanninkhof R, Sweeney C, Feely RA, et al. 2009. Climatological mean and decadal change in surface ocean pCO_2, and net sea–air CO_2 flux over the global oceans. *Deep-Sea Res. II* 56:554–77

Takahashi T, Sweeney C, Hales B, Chipman D, Newberger T, et al. 2012. The changing carbon cycle in the Southern Ocean. *Oceanography* 25(3):26–37

Talley LD, Feely RA, Sloyan BM, Wanninkhof R, Baringer MO, et al. 2016. Changes in ocean heat, carbon content, and ventilation: a review of the first decade of GO-SHIP global repeat hydrography. *Annu. Rev. Mar. Sci.* 8:185–215

Tanhua T, Kortzinger A, Friis K, Waugh DW, Wallace DWR. 2007. An estimate of anthropogenic CO_2 inventory from decadal changes in oceanic carbon content. *PNAS* 104:3037–42

Verdy A, Mazloff MR. 2017. A data assimilating model for estimating Southern Ocean biogeochemistry. *J. Geophys. Res. Oceans* 122:6968–88

Wallace DWR. 2001. Storage and transport of excess CO_2 in the oceans: the JGOFS/WOCE global CO_2 survey. In *Ocean Circulation and Climate*, ed. G Siedler, J Church, J Gould, pp. 489–524. San Diego, CA: Academic

Wanninkhof R, Asher WE, Ho DT, Sweeney C, McGillis WR. 2009. Advances in quantifying air-sea gas exchange and environmental forcing. *Annu. Rev. Mar. Sci.* 1:213–44

Wanninkhof R, Doney SC, Bullister JL, Levine NM, Warner M, Gruber N. 2010. Detecting anthropogenic CO_2 changes in the interior Atlantic Ocean between 1989 and 2005. *J. Geophys. Res.* 115:1–25

Wanninkhof R, Park GH, Takahashi T, Sweeney C, Feely R, et al. 2013. Global ocean carbon uptake: magnitude, variability and trends. *Biogeosciences* 10:1983–2000

Watson AJ, Bakker DCE, Ridgewell AJ, Boyd PW, Law CS. 2000. Effect of iron supply on Southern Ocean CO_2 uptake and implications for glacial atmospheric CO_2. *Nature* 407:730–33

Waugh DW, Hall TM, McNeil BI, Key R, Matear RJ. 2006. Anthropogenic CO_2 in the oceans estimated using transit time distributions. *Tellus B* 58:376–89

Waugh DW, Primeau F, Devries T, Holzer M. 2013. Recent changes in the ventilation of the southern oceans. *Science* 339:568–70

Williams NL, Juranek LW, Feely RA, Russell JL, Johnson KS, Hales B. 2018. Assessment of the carbonate chemistry seasonal cycles in the Southern Ocean from persistent observational platforms. *J. Geophys. Res. Oceans* 123:4833–52

Woosley RJ, Millero FJ, Wanninkhof R. 2016. Rapid anthropogenic changes in CO_2 and pH in the Atlantic Ocean: 2003–2014. *Glob. Biogeochem. Cycles* 30:70–90

Xue L, Gao L, Cai W-J, Yu W, Wei M. 2015. Response of sea surface fugacity of CO_2 to the SAM shift south of Tasmania: regional differences. *Geophys. Res. Lett.* 42:3973–79

Yeager S, Danabasoglu G, Rosenbloom N, Strand W, Bates S, et al. 2018. Predicting near-term changes in the Earth system: a large ensemble of initialized decadal prediction simulations using the Community Earth System Model. *Bull. Am. Meteor. Soc.* 99:1867–86